Electronic Supporting Information

Modulation of Luminescent Behaviour in *N*-Heterocyclic Thione

Joginder Singh,[a] Gopendra Muduli,[a] Sabari Veerapathiran,[a] Arushi Rawat, [b] Muneshwar Nandeshwar, [a] Abhilash Sahu,[b] Kohsuke Matsumoto,[b] Osamu Tsutsumi, [b] and Ganesan Prabusankar *[a]

[a] Mr. Joginder Singh, Mr. Gopendra Muduli, Dr. Sabari Veerapathiran, Dr. Muneshwar Nandeshwar and Prof. Dr. Ganesan Prabusankar, Organometallics and Materials Chemistry Lab, Department of Chemistry, Indian Institute of Technology Hyderabad, Kandi, Sangareddy, Telangana, India-502285

E-mail: prabu@chy.iith.ac.in

[b] Ms. Arushi Rawat, Abhilash Sahu, Kohsuke Matsumoto, and Prof. Dr. Osamu Tsutsumi, Department of Applied Chemistry, Ritsumeikan University, Kusatsu 525-8577, Japan.

E-Mail: tsutsumi@sk.ritsumei.ac.jp

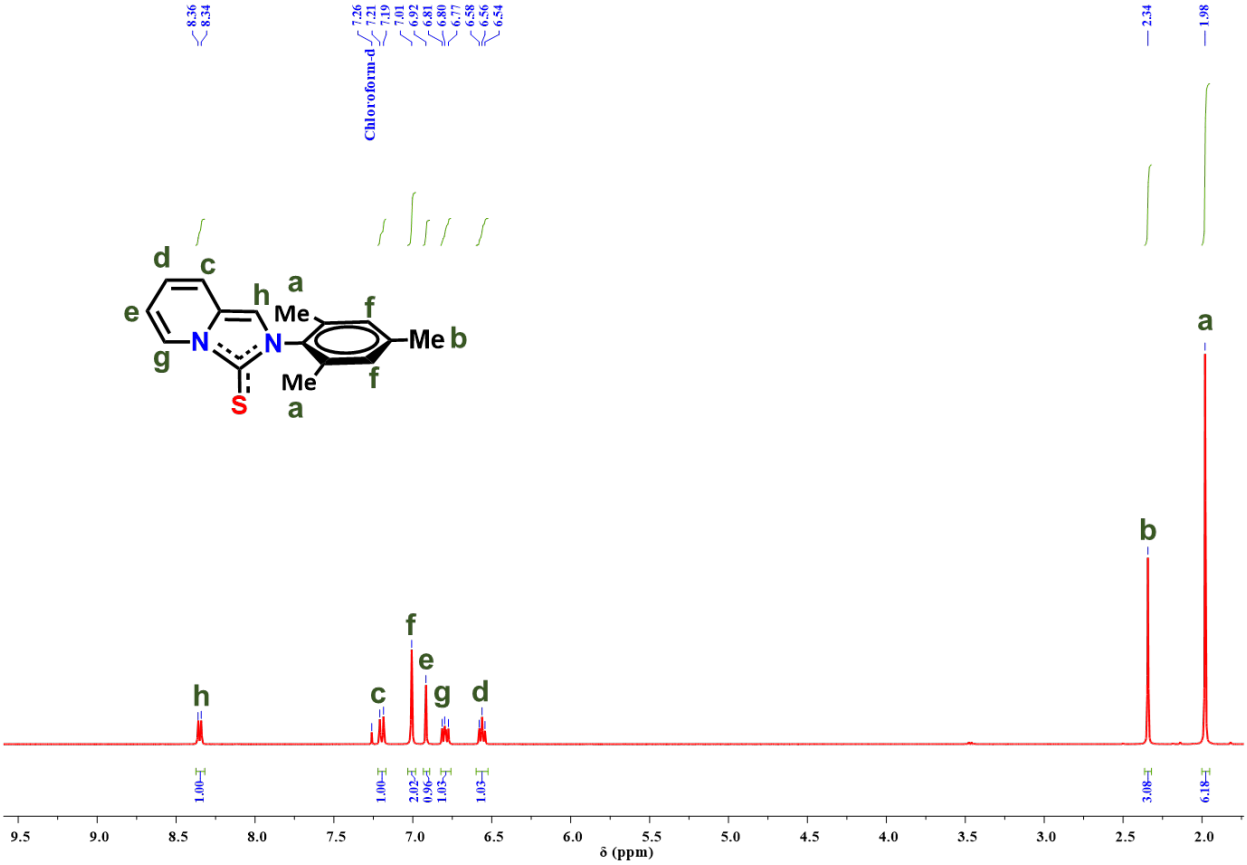

Figure S1: ^{1}H NMR spectrum of **MPIT** in $CDCl_3$ at 25 ^{o}C.

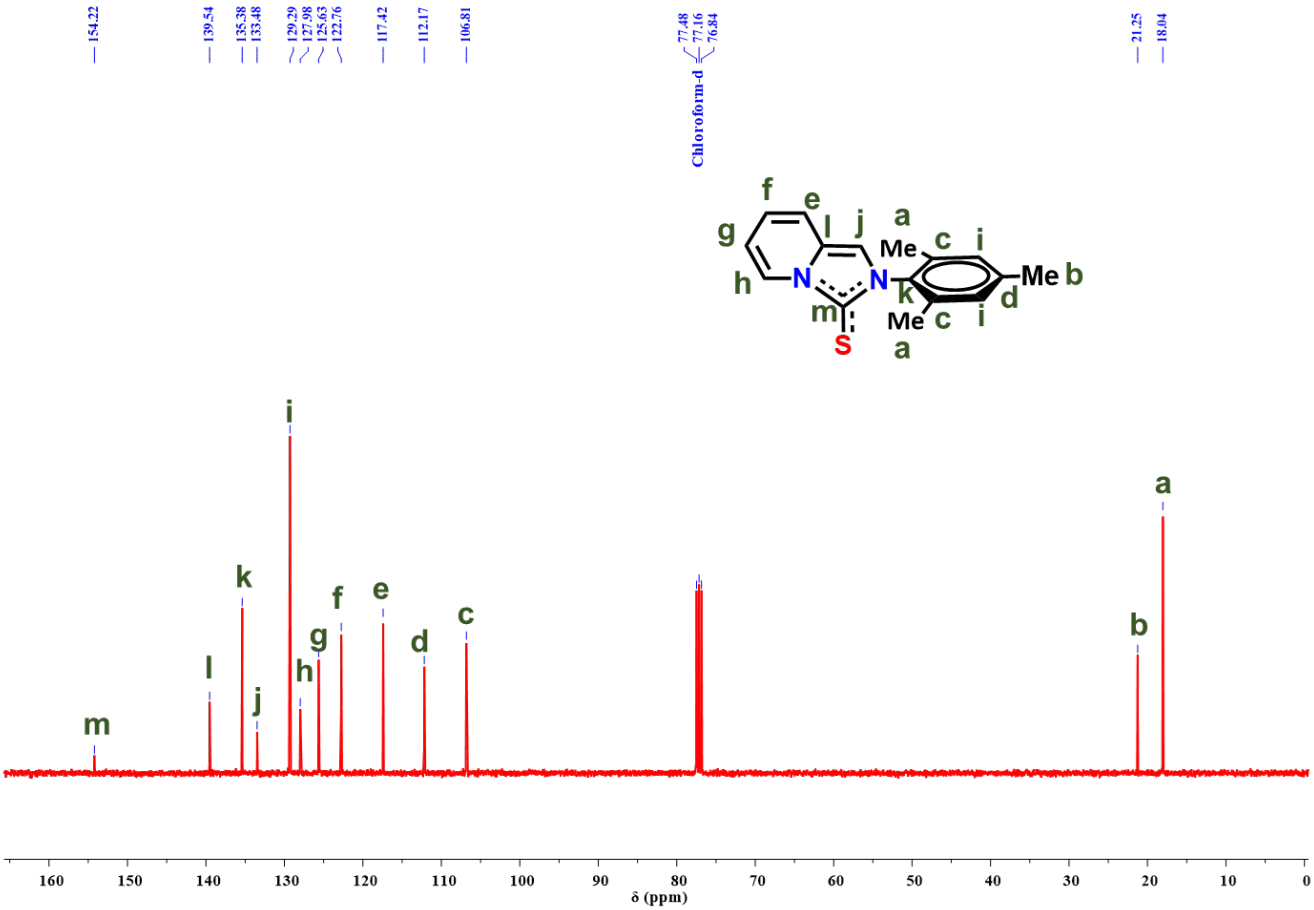

Figure S2: ^{13}C NMR spectrum of **MPIT** in $CDCl_3$ at 25 °C.

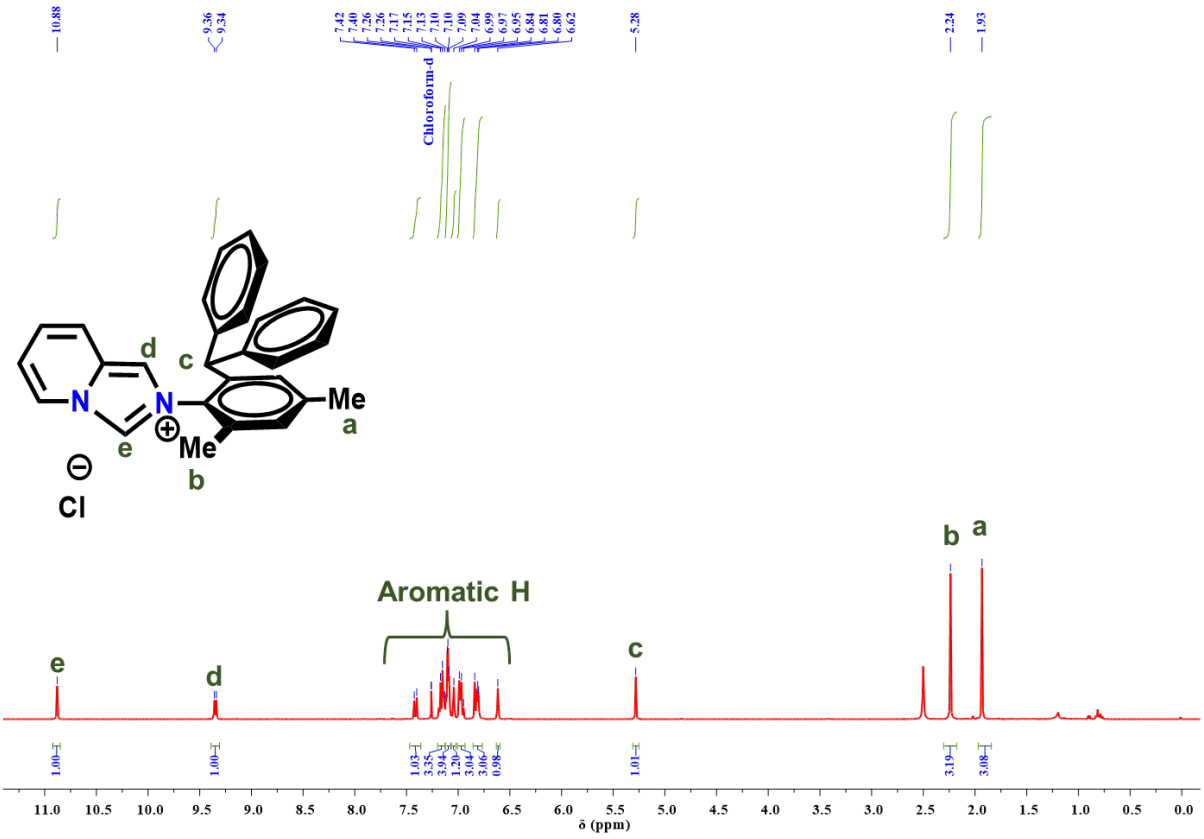

Figure S3: ^{1}H NMR spectrum of **L²** in $CDCl_3$ at 25 °C.

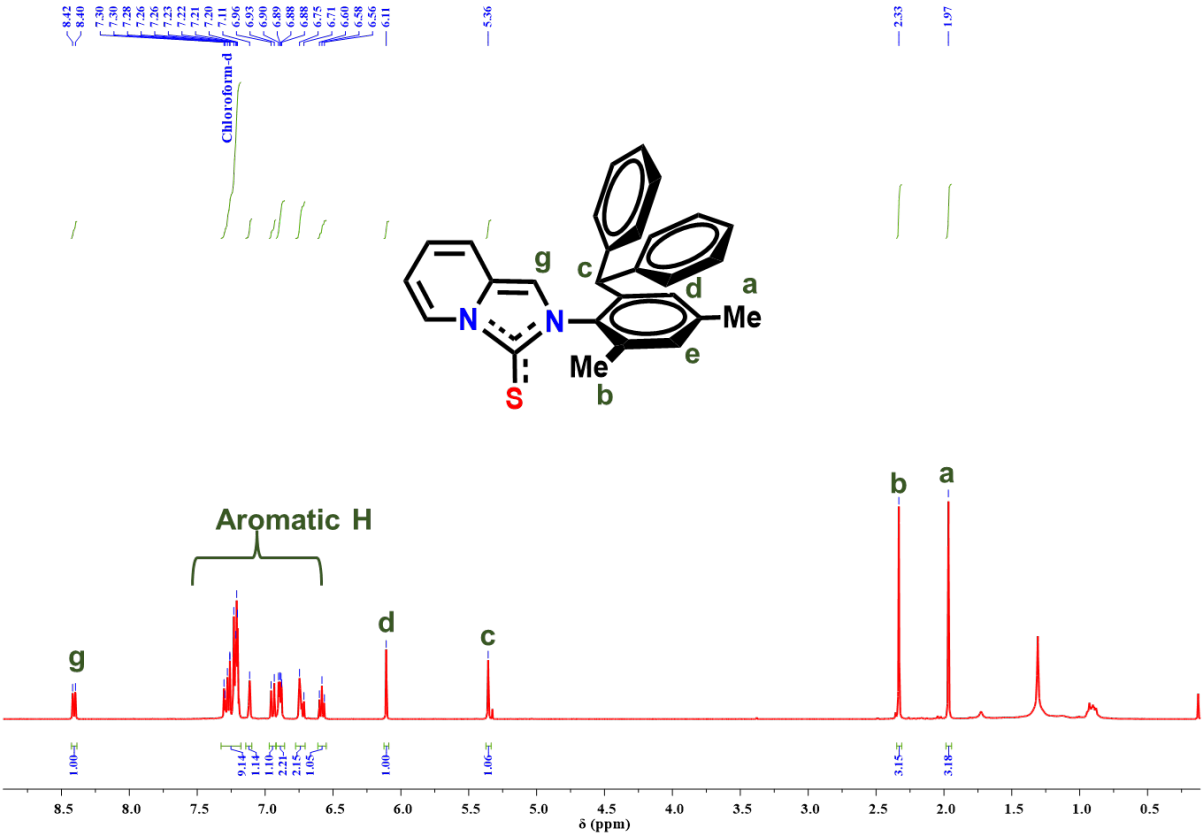

Figure S4: ^{1}H NMR spectrum of **DPPIT** in $CDCl_3$ at 25 °C.

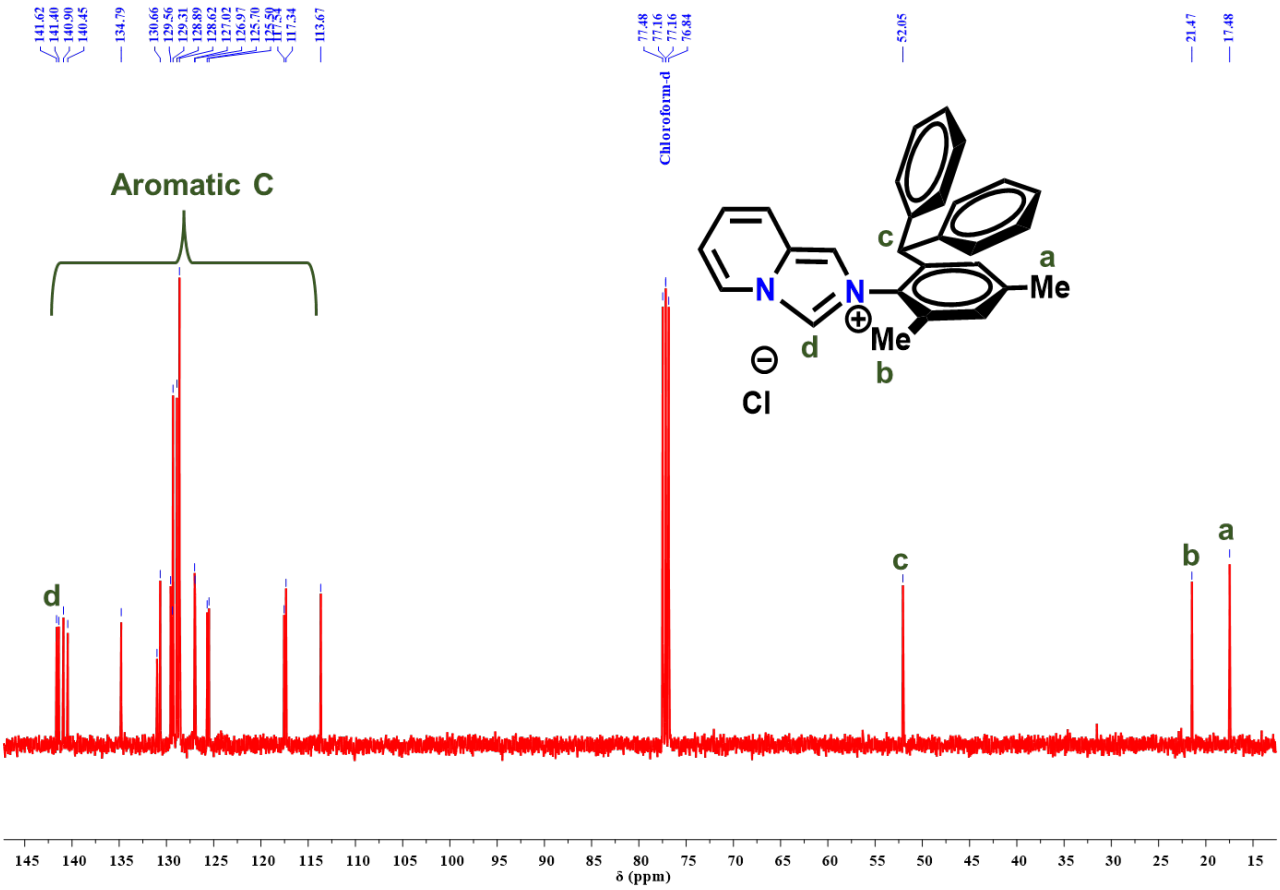

Figure S5: ^{13}C NMR spectrum of **L²** in $CDCl_3$ at 25 °C.

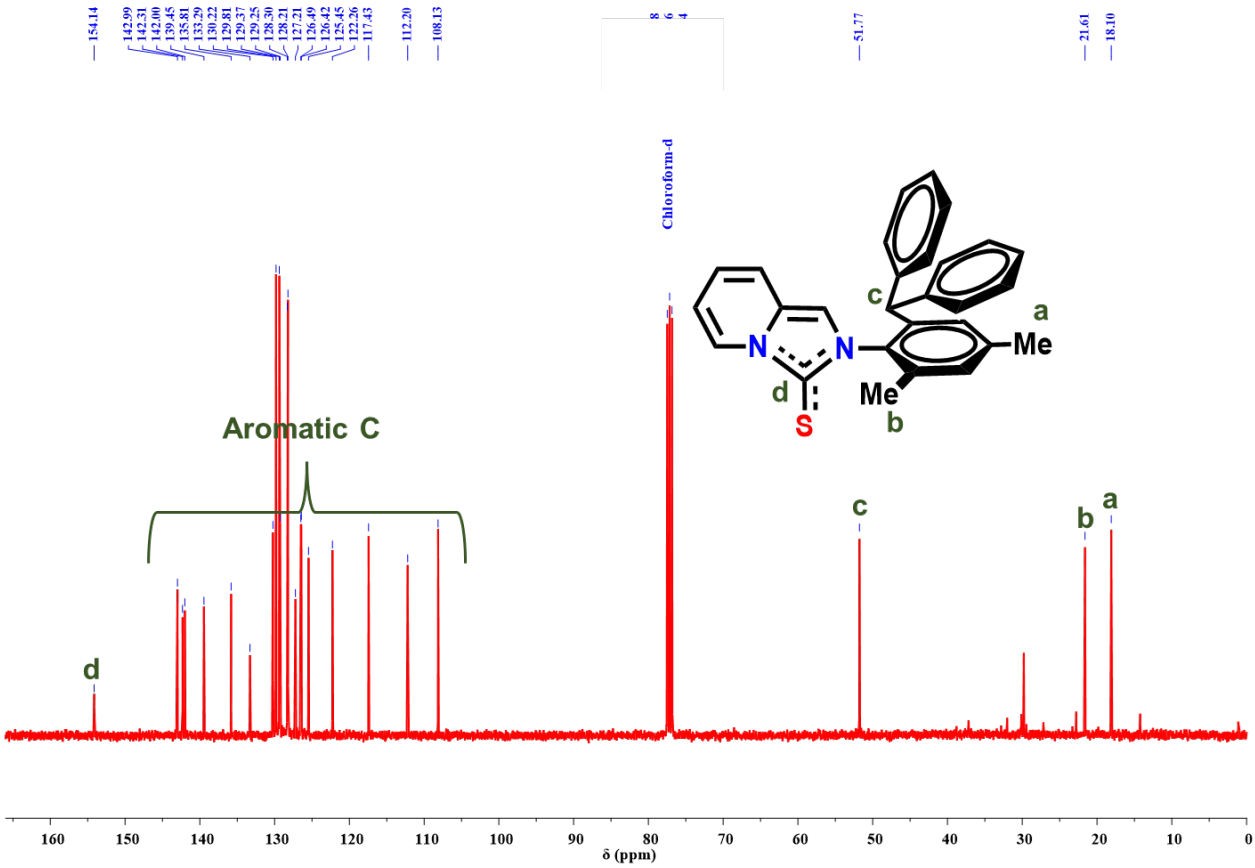

Figure S6: ^{13}C NMR spectrum of **DPPIT** in $CDCl_3$ at 25 °C.

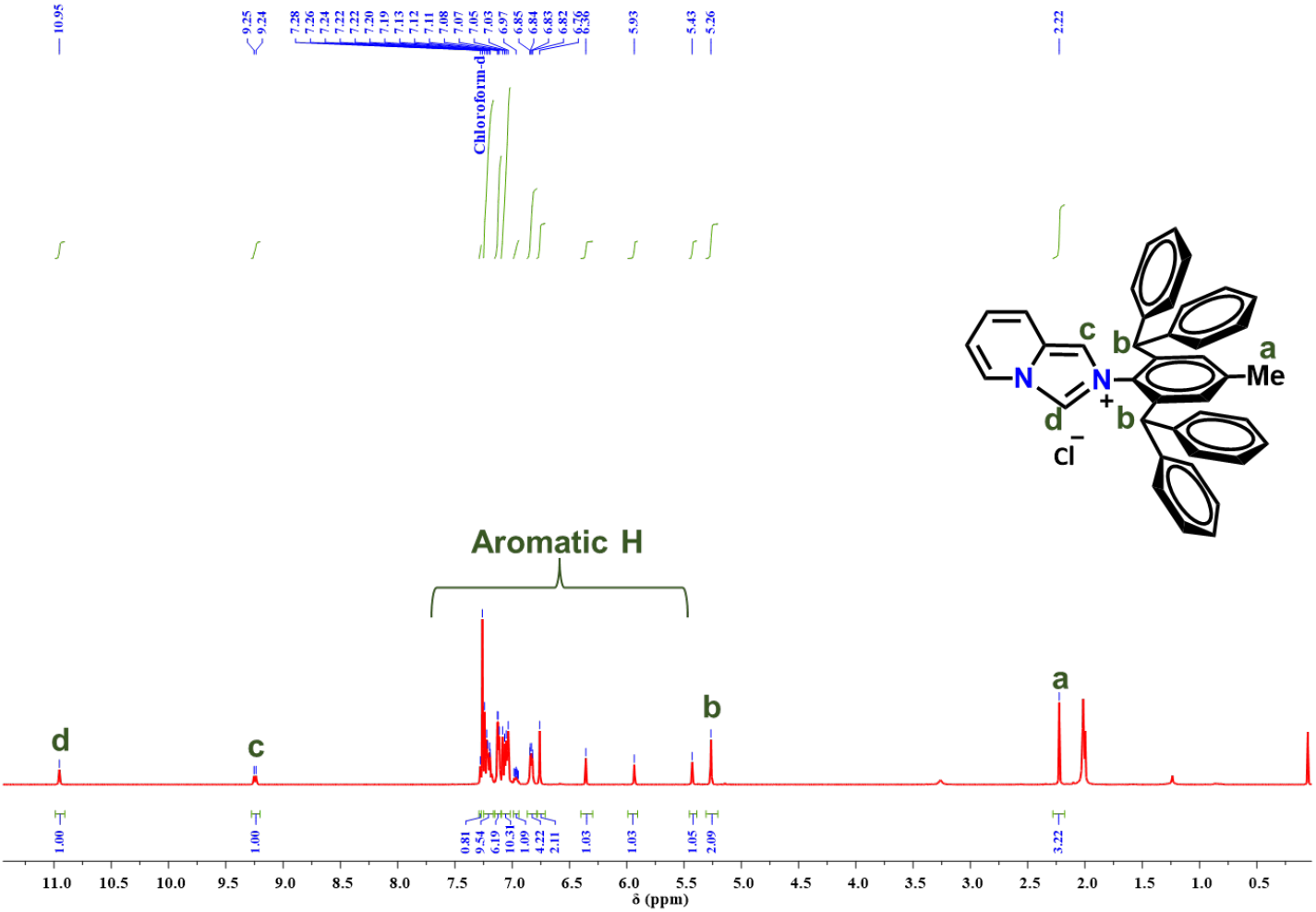

Figure S7: ^{1}H NMR spectrum of **L^{3}** in $CDCl_3$ at 25 ^{o}C.

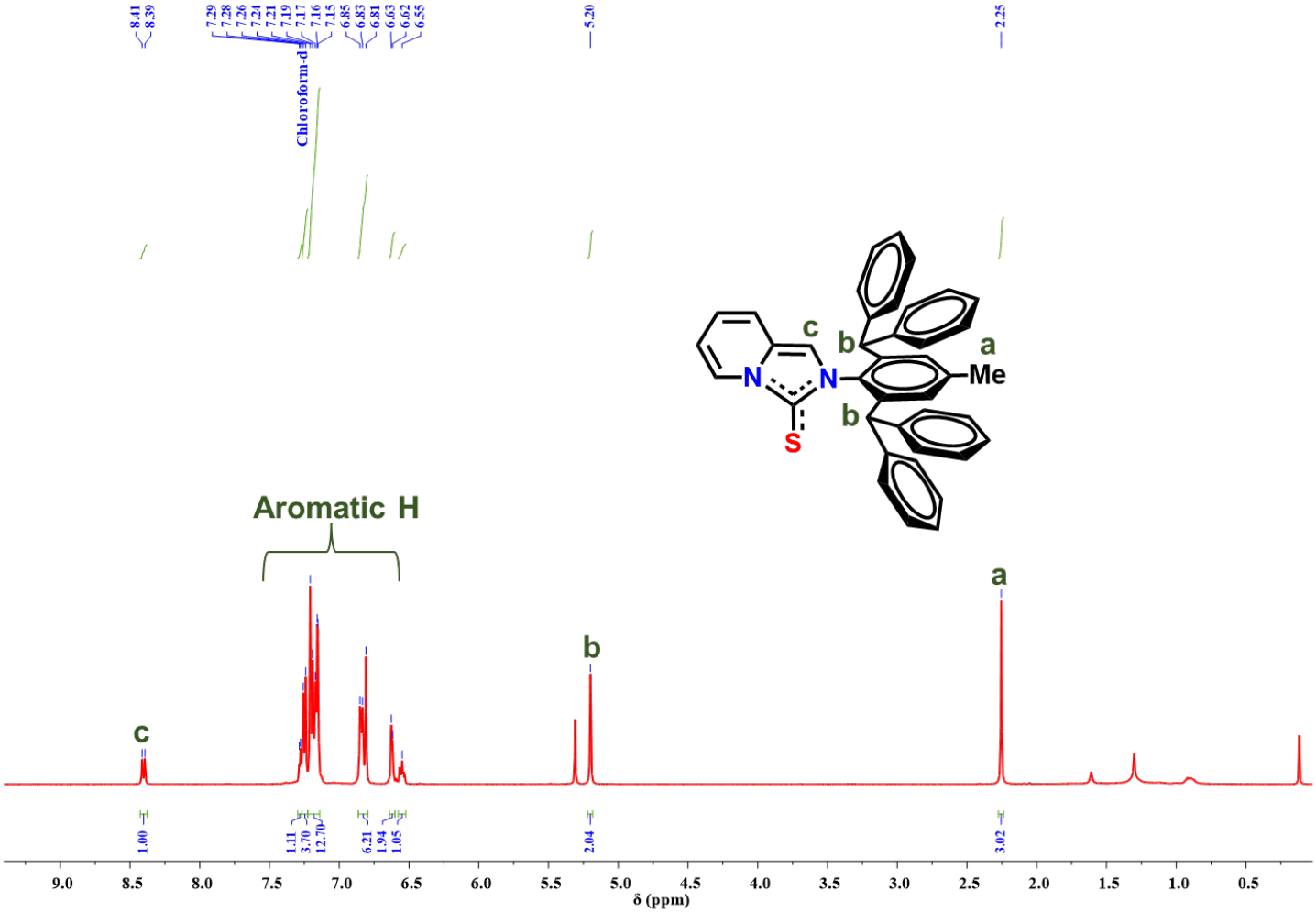

Figure S8: ^{1}H NMR spectrum of **TPPIT** in $CDCl_3$ at 25 °C.

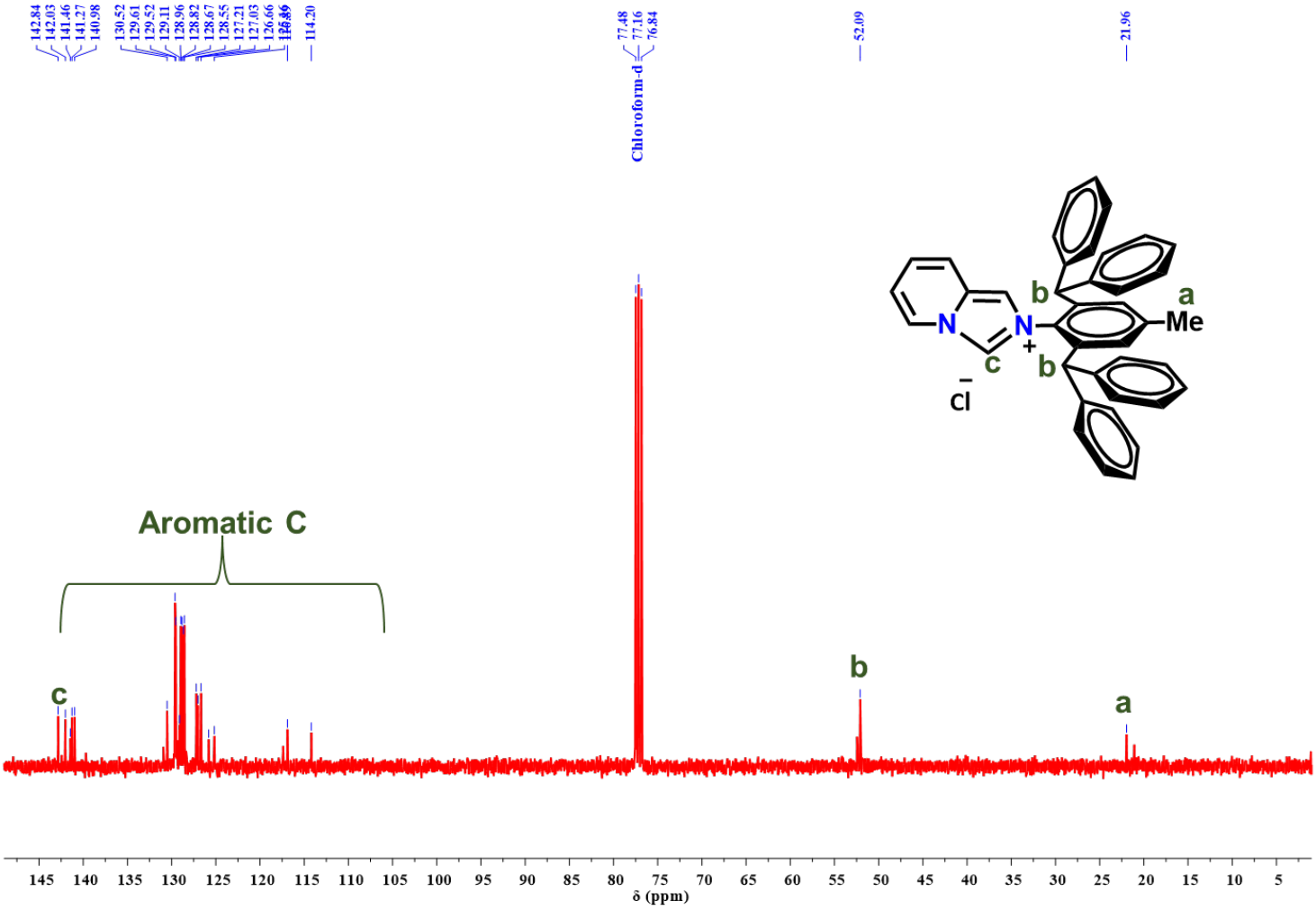

Figure S9: ^{13}C NMR spectrum of **L³** in $CDCl_3$ at 25 °C.

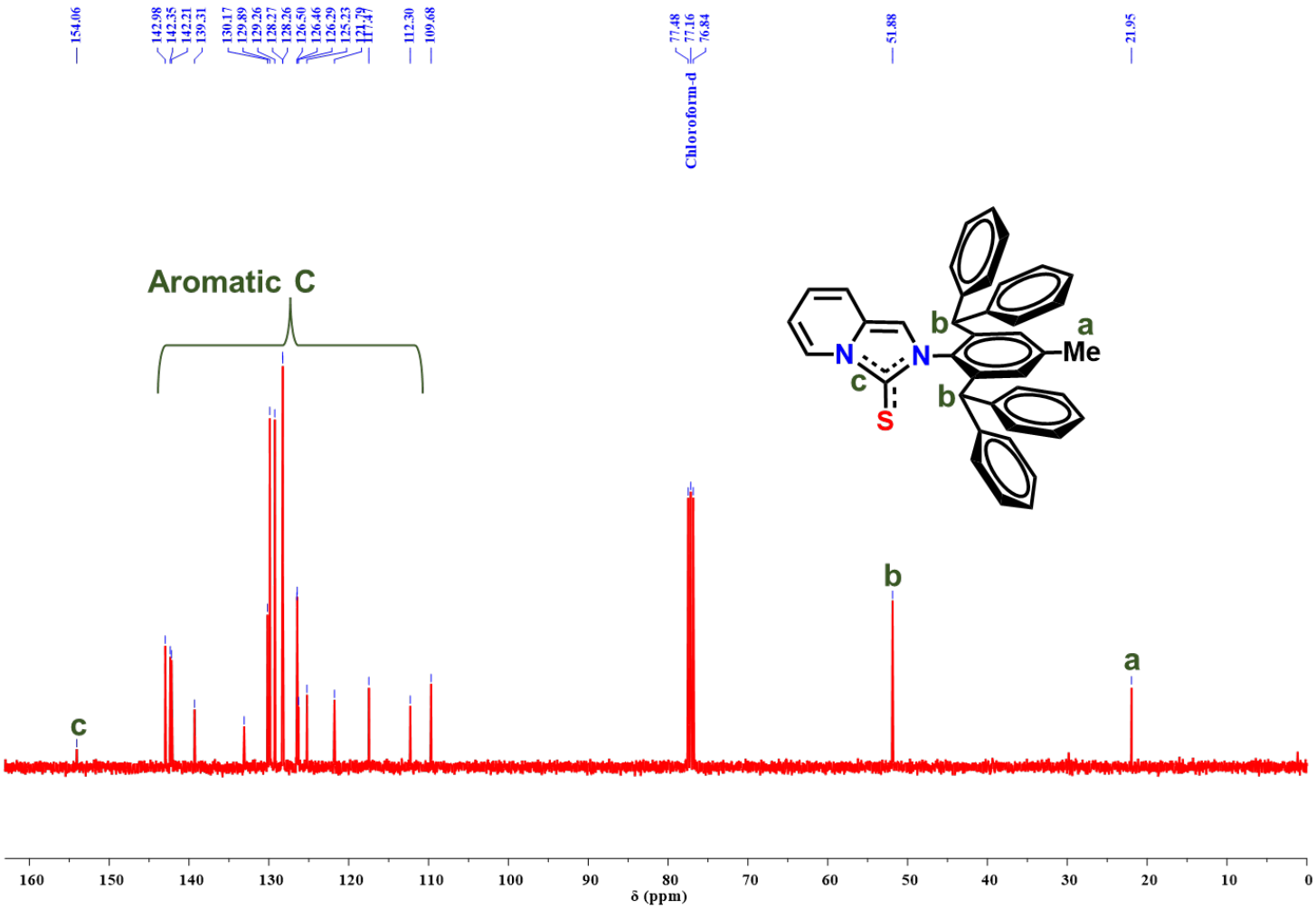

Figure S10: ^{13}C NMR spectrum of **TPPIT** in $CDCl_3$ at 25 °C.

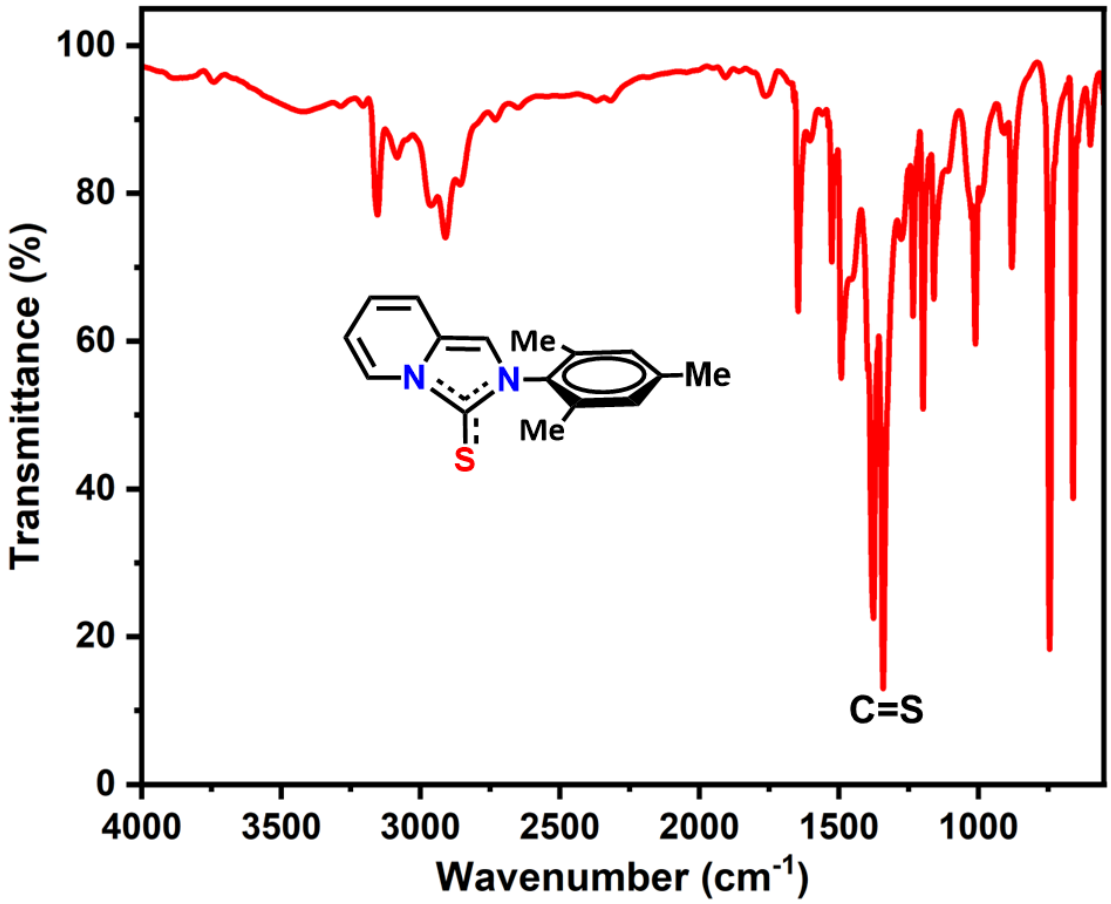

Figure S11: FT-IR spectrum of **MPIT** at 25 ºC (ATR method).

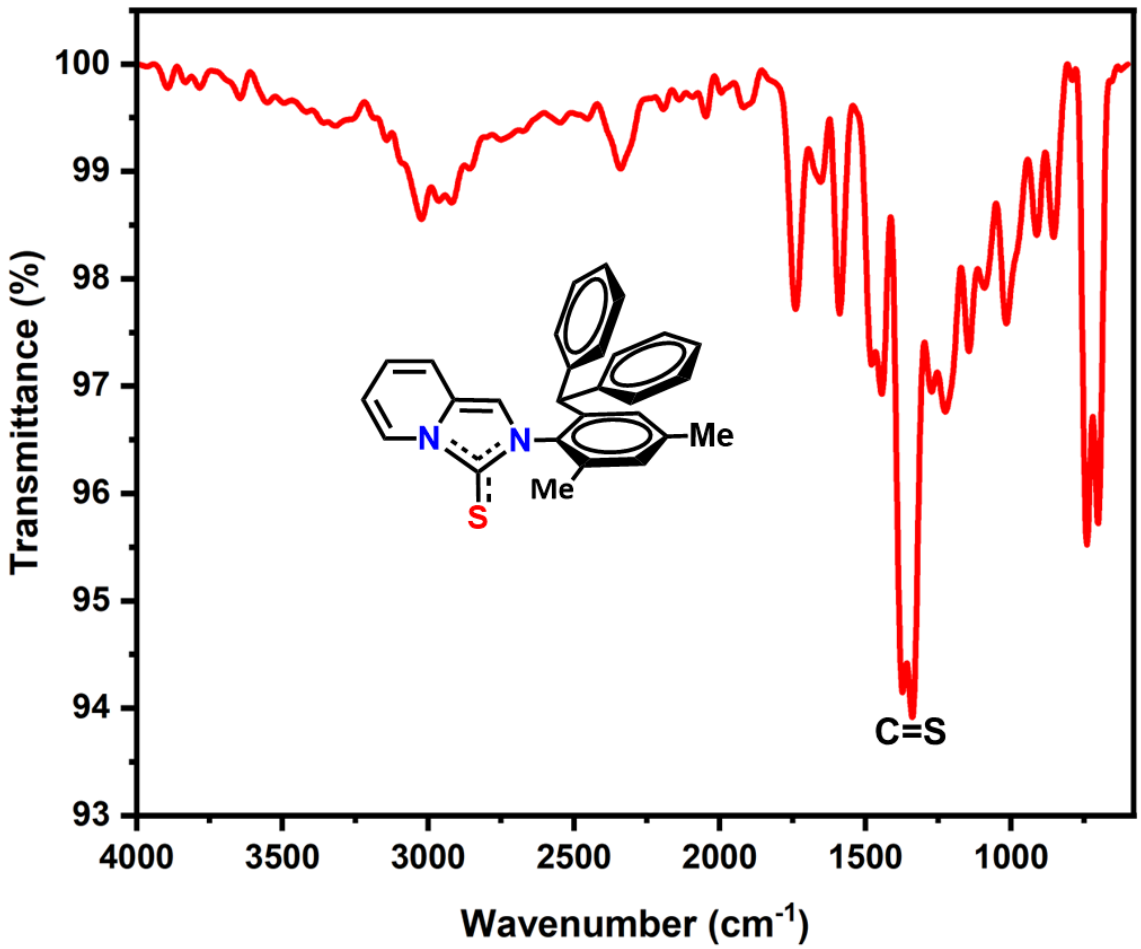

Figure S12: FT-IR spectrum of **DPPIT** at 25 ºC (ATR method).

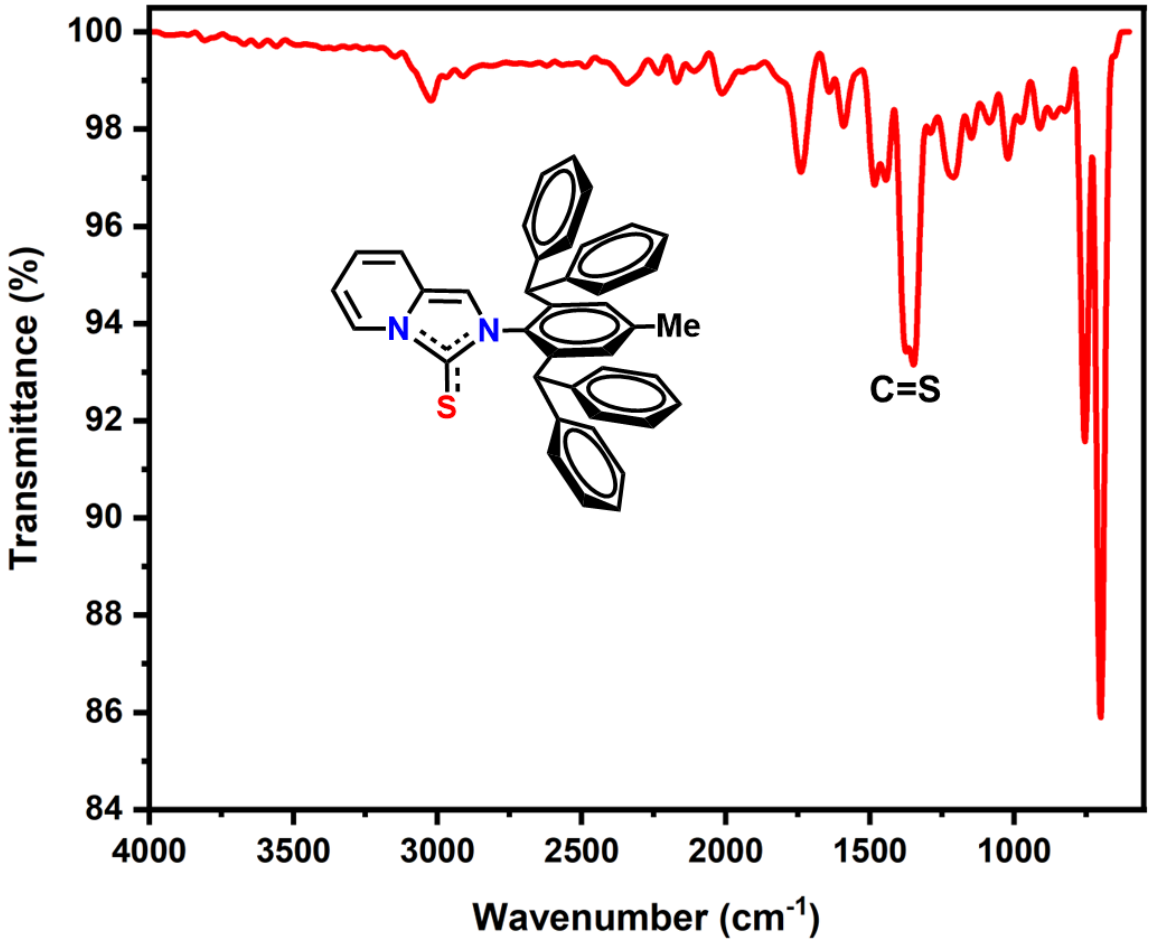

Figure S13: FT-IR spectrum of **TPPIT** at 25 ºC (ATR method).

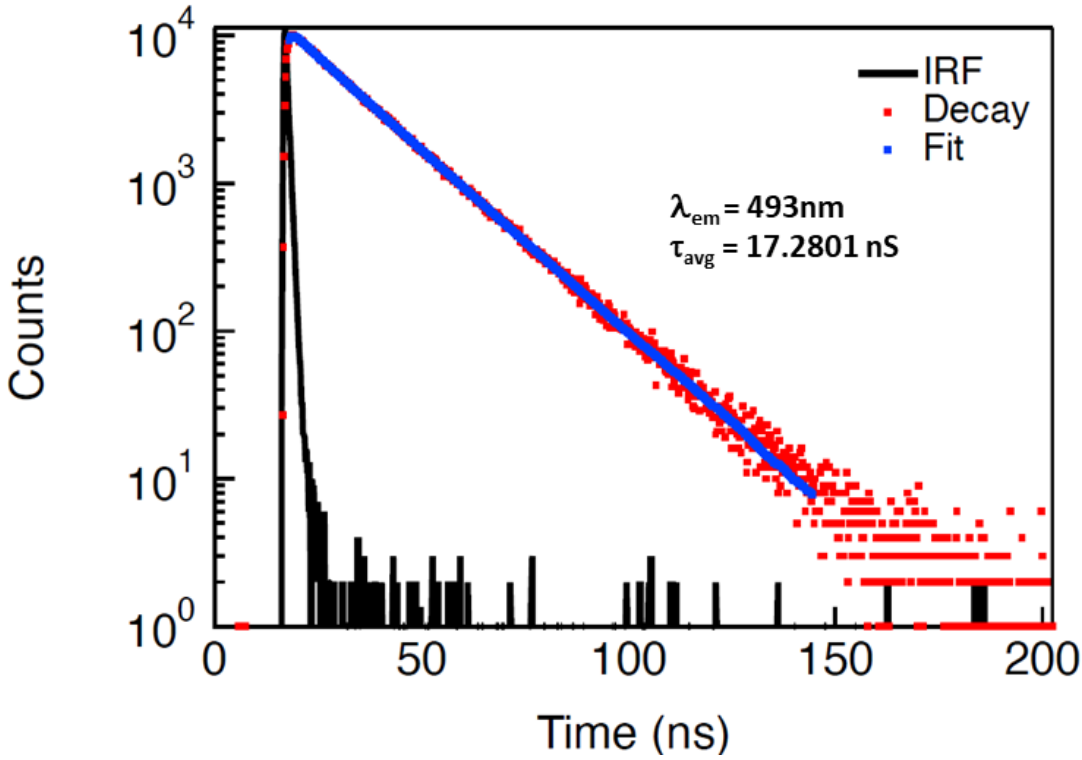

Figure S14: Lifetime measurement graph of **MPIT** in CH_2Cl_2.

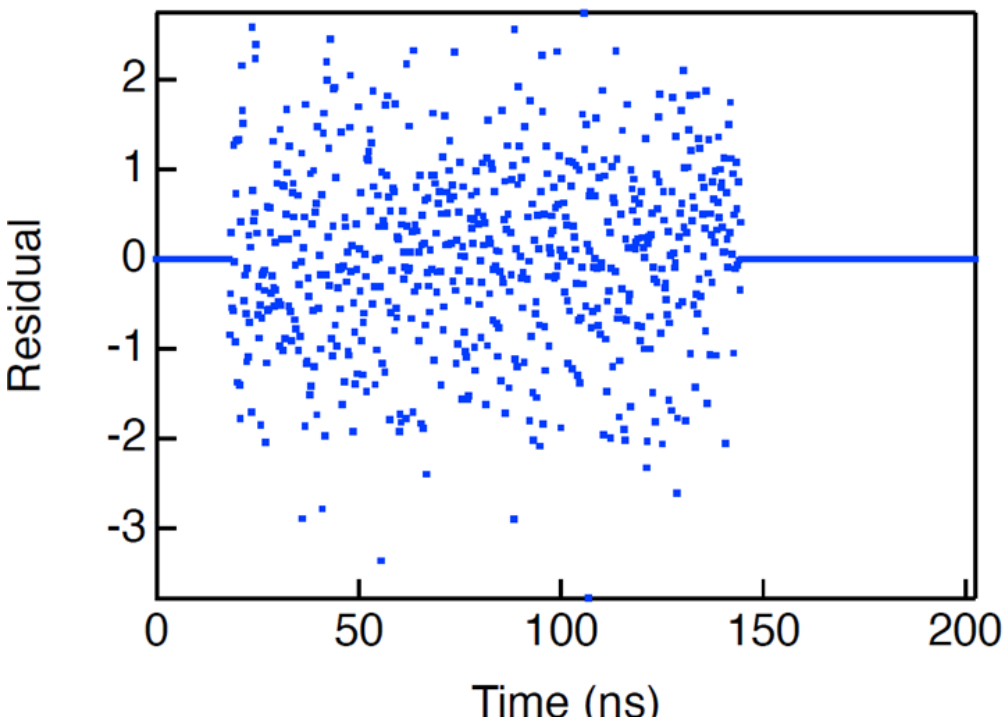

Figure S15: Residual graph of lifetime measurement of **MPIT** in CH_2Cl_2.

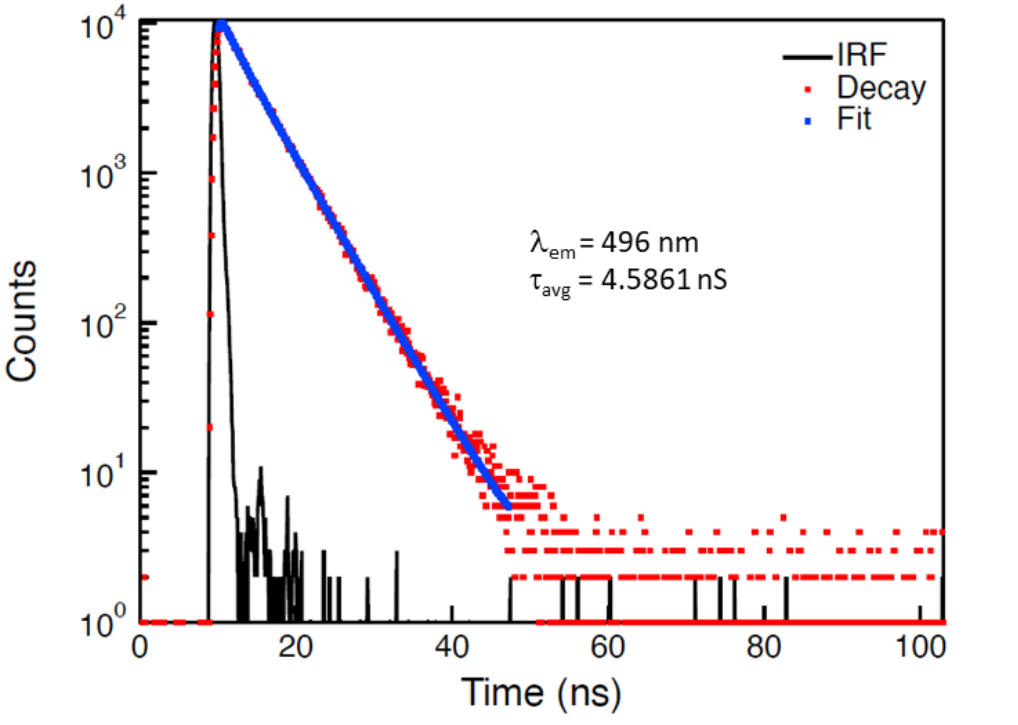

Figure S16: Lifetime measurement graph of **MPIT** in crystalline state.

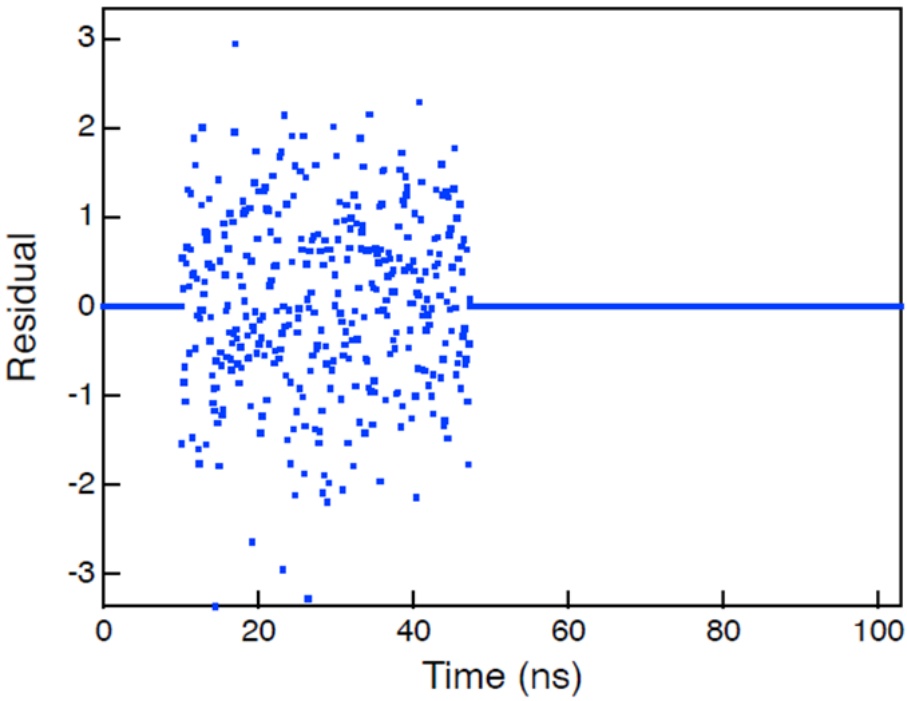

Figure S17: Residual graph of lifetime measurement of **MPIT** in crystalline state.

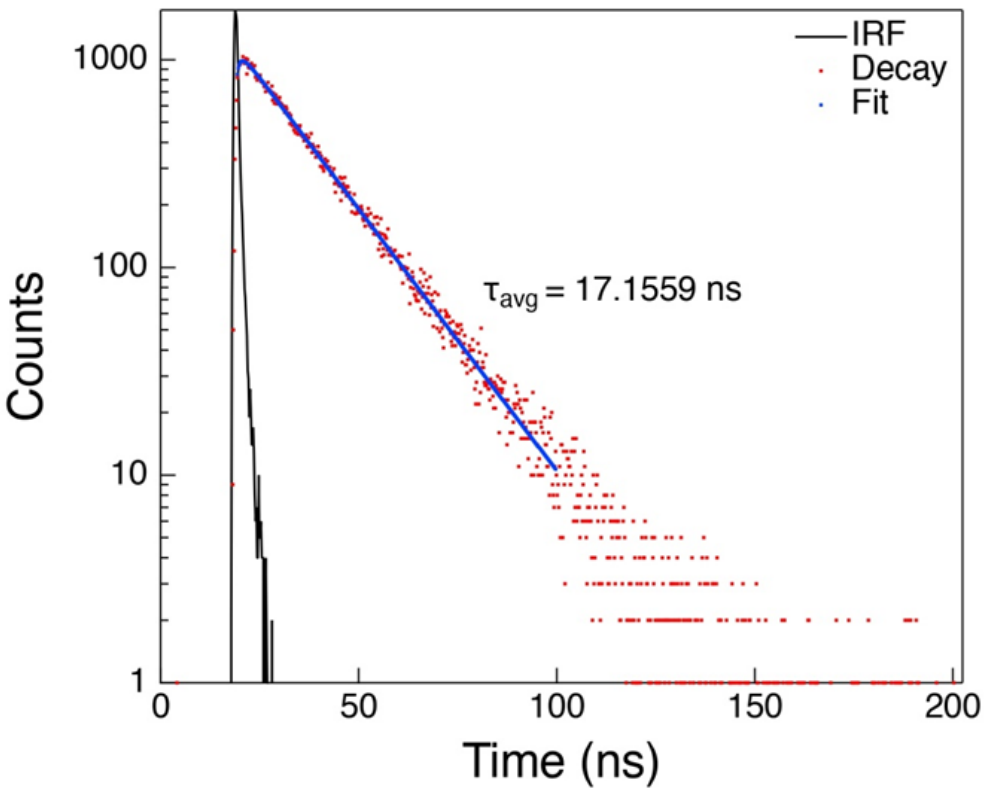

Figure S18: Lifetime measurement graph of **DPPIT** in CH_2Cl_2.

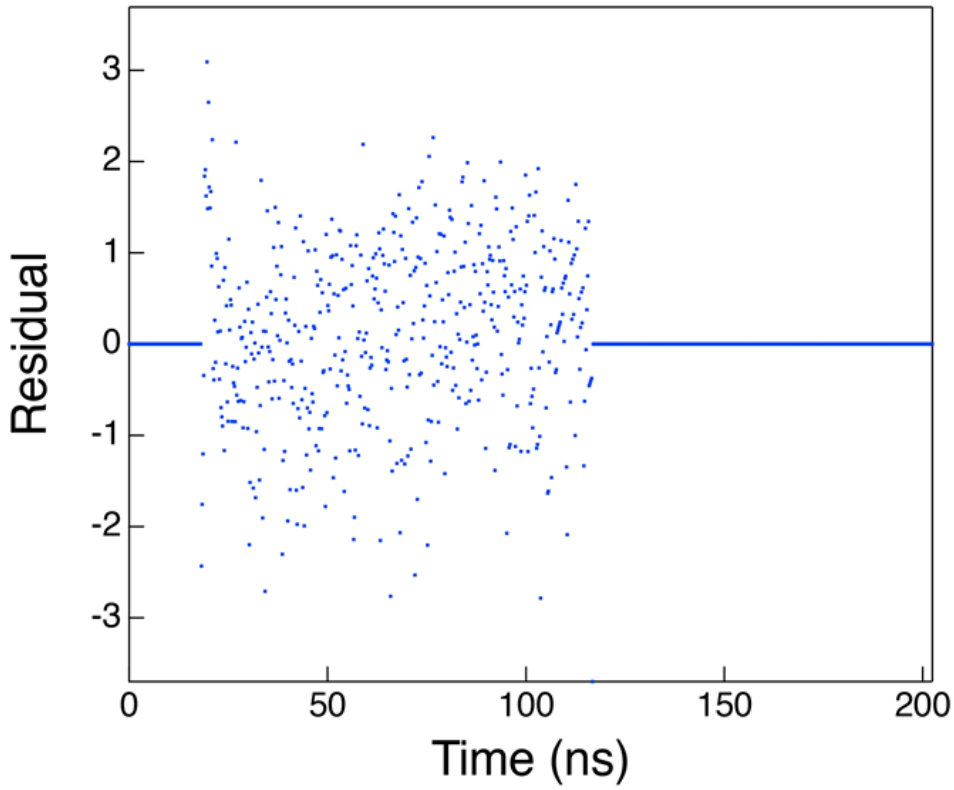

Figure S19: Residual graph of lifetime measurement of **DPPIT** in CH_2Cl_2.

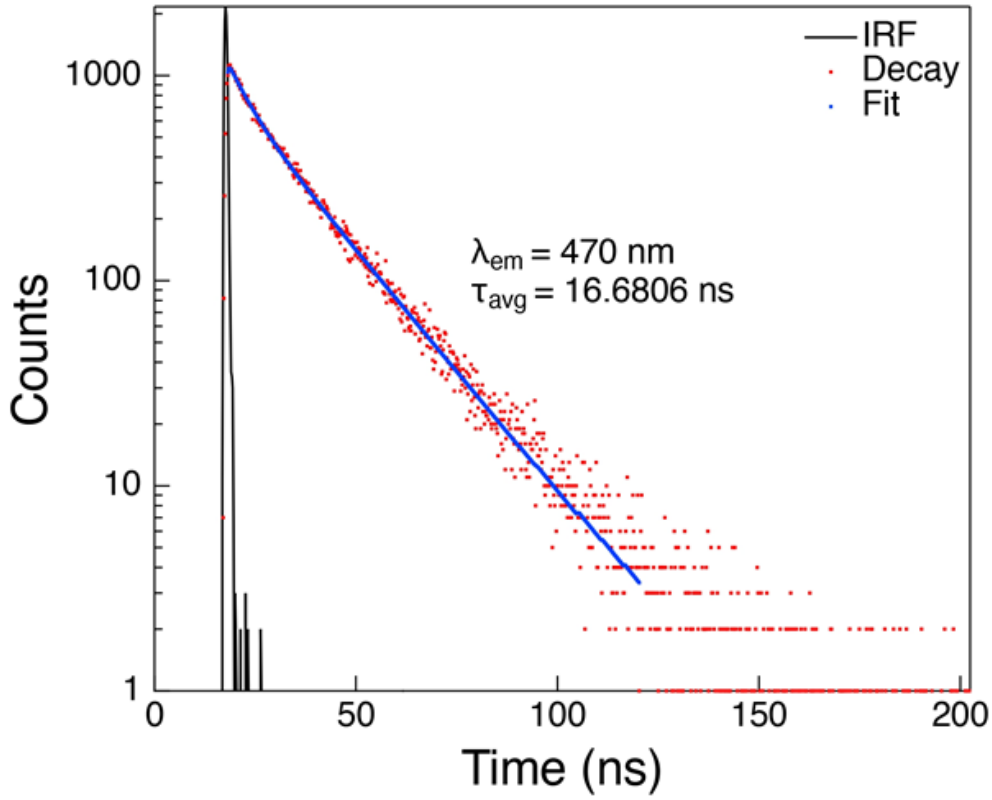

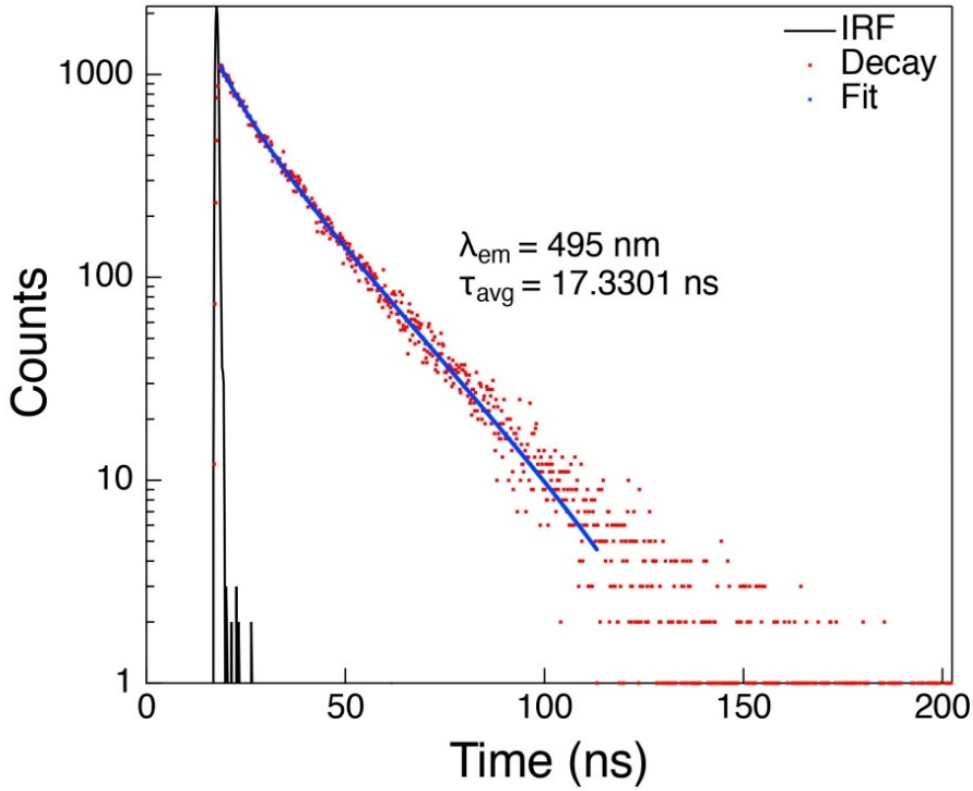

Figure S20: Lifetime measurement graphs of **DPPIT** in crystalline state.

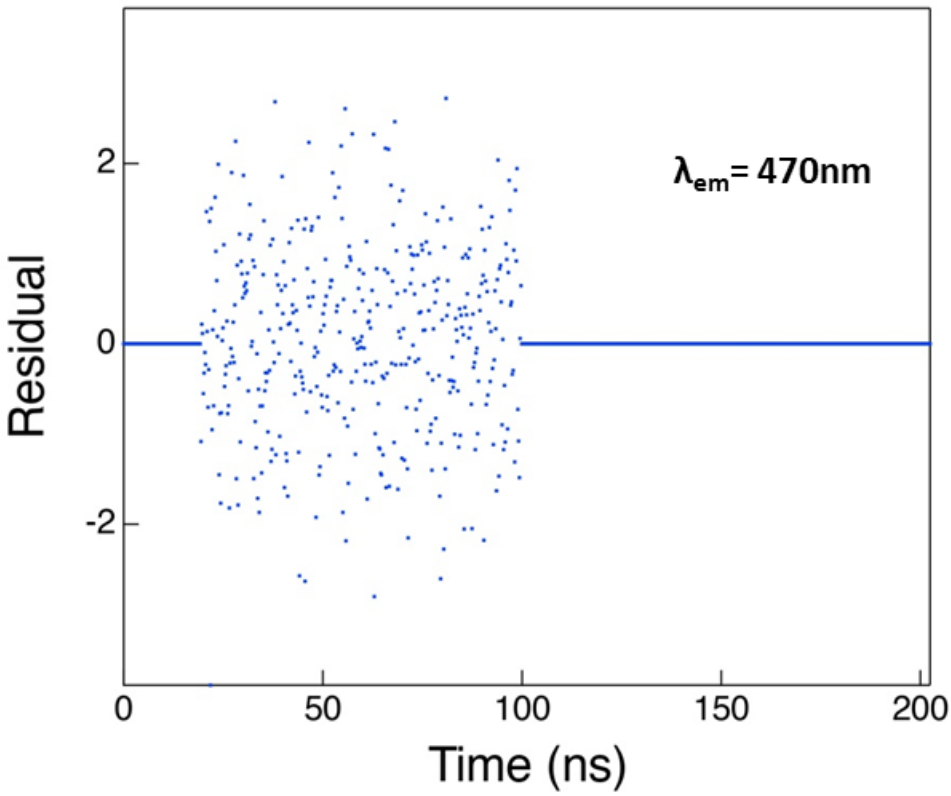

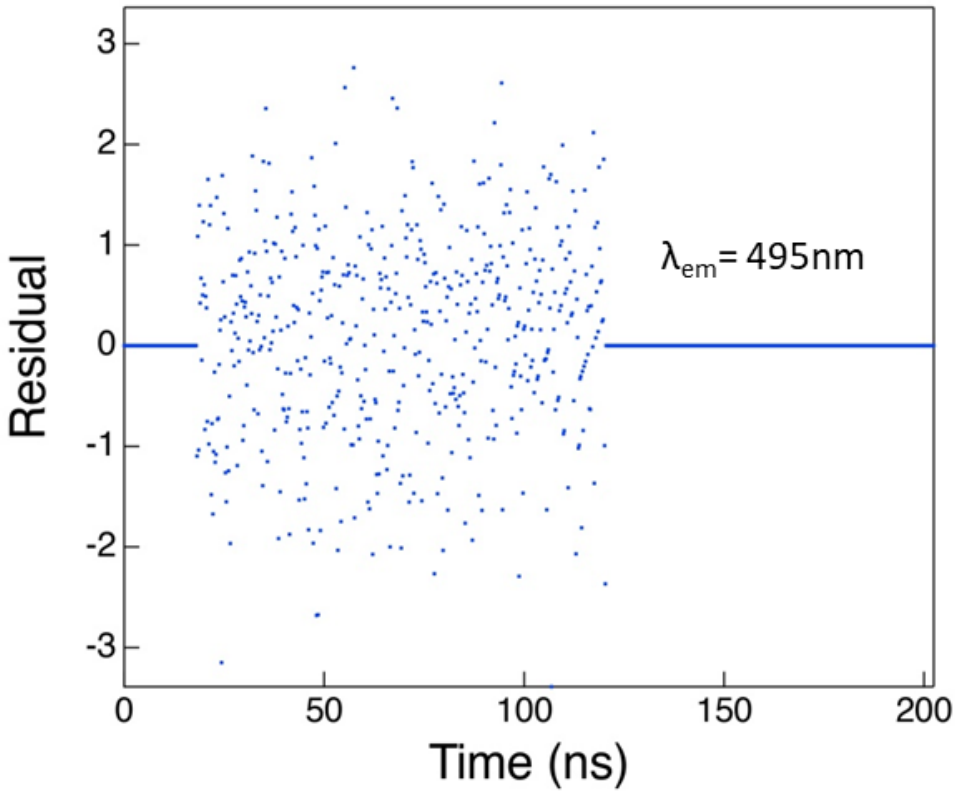

Figure S21: Residual graphs of lifetime measurement of **DPPIT** in crystalline state.

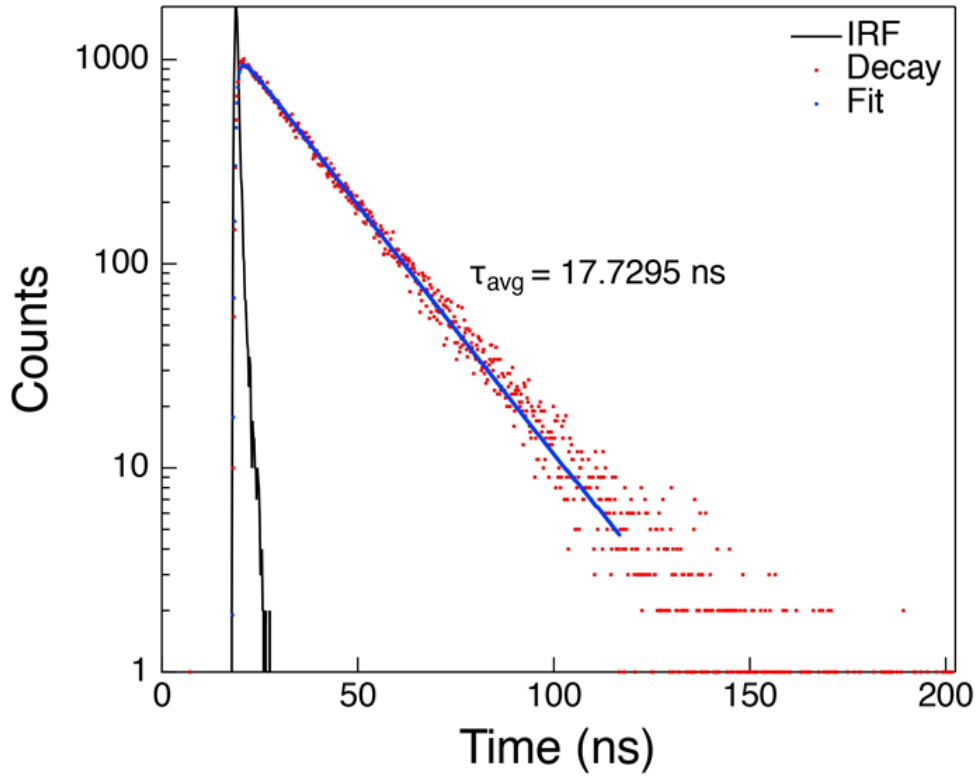

Figure S22: Lifetime measurement graph of **TPPIT** in CH_2Cl_2.

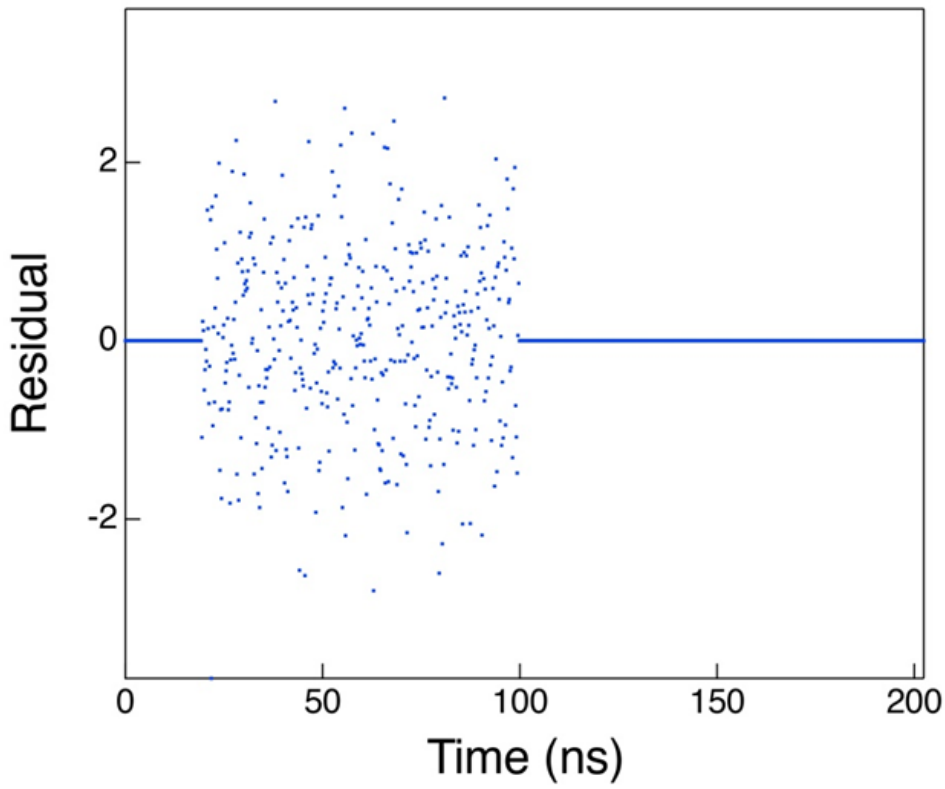

Figure S23: Residual graph of lifetime measurement of **TPPIT** in CH_2Cl_2.

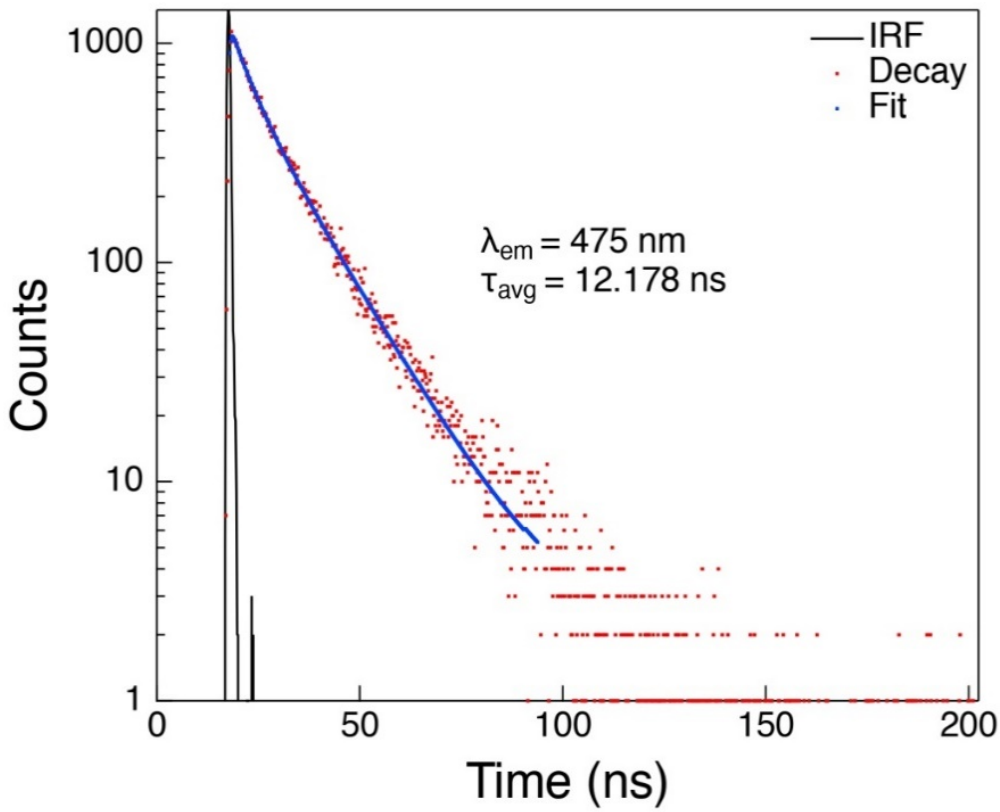

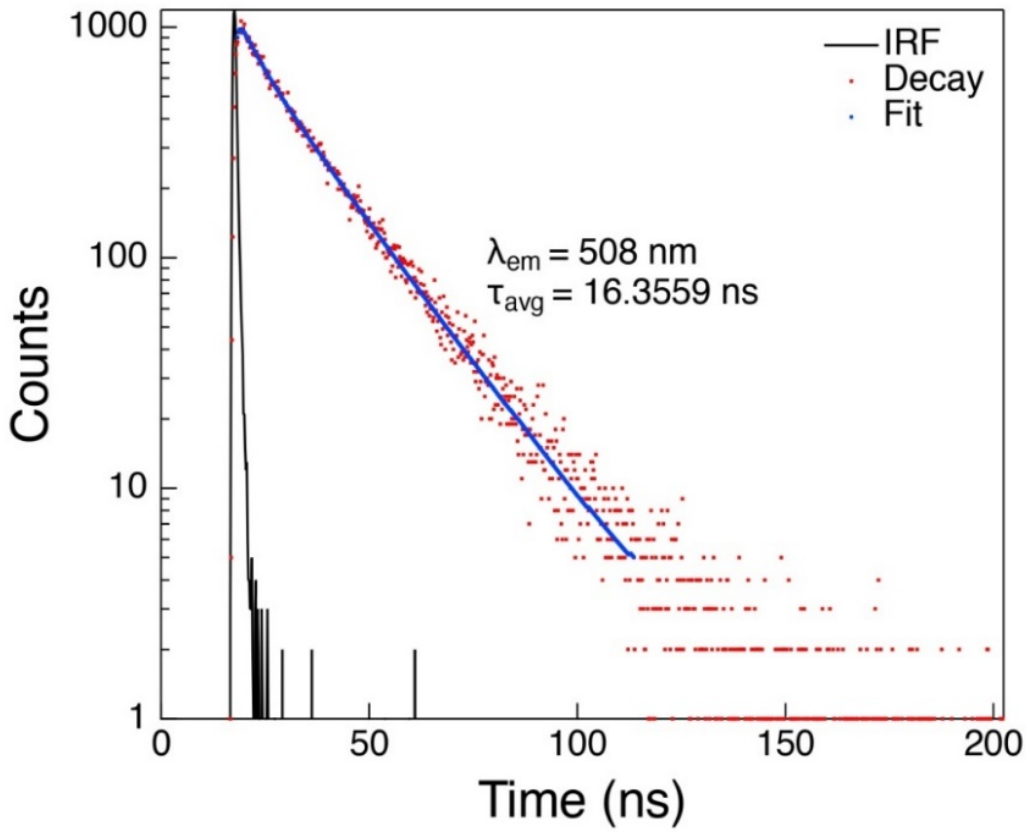

Figure S24: Lifetime measurement graphs of **TPPIT** in crystalline state.

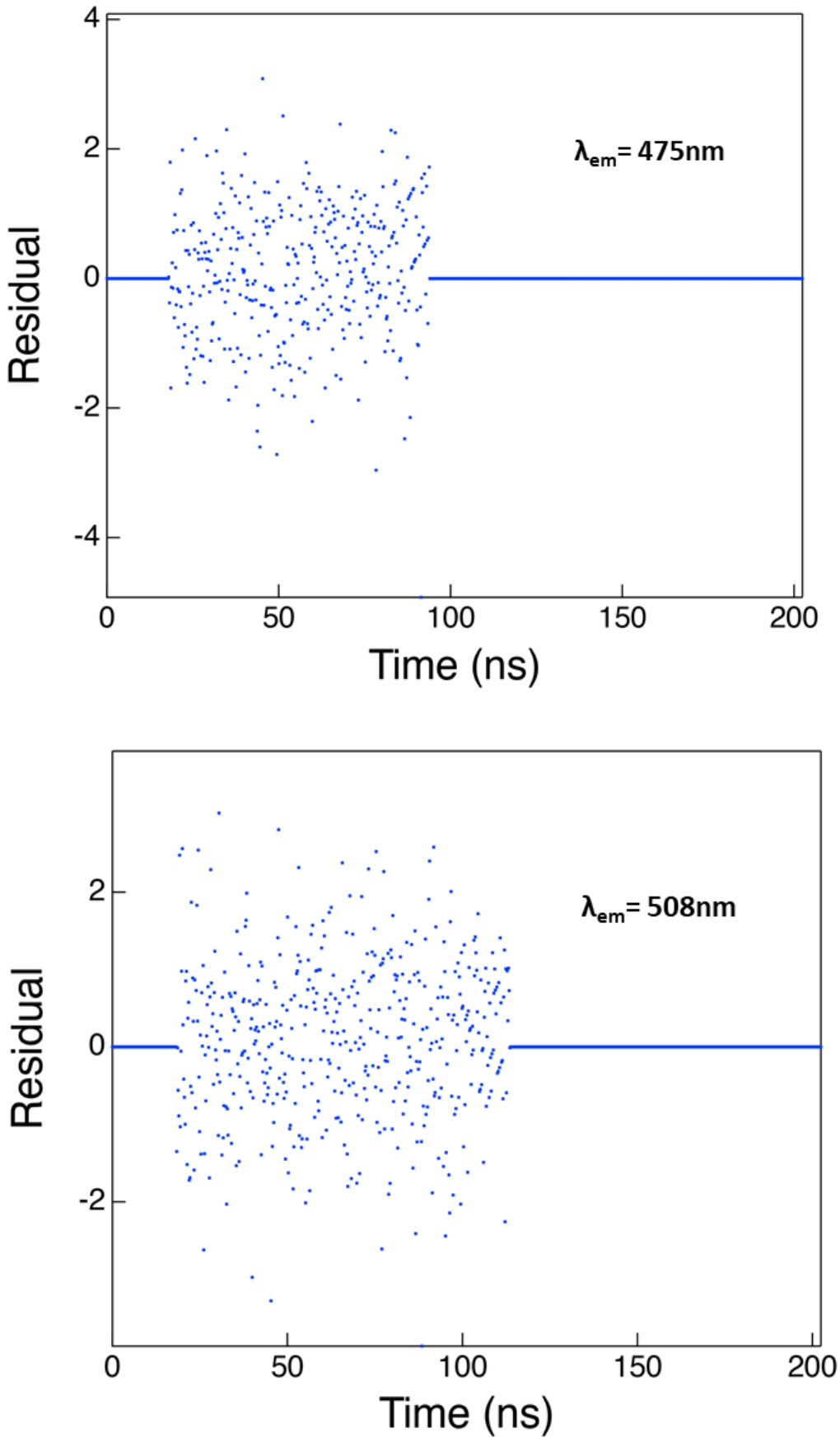

Figure S25: Residual graphs of lifetime measurement of **TPPIT** in crystalline state.

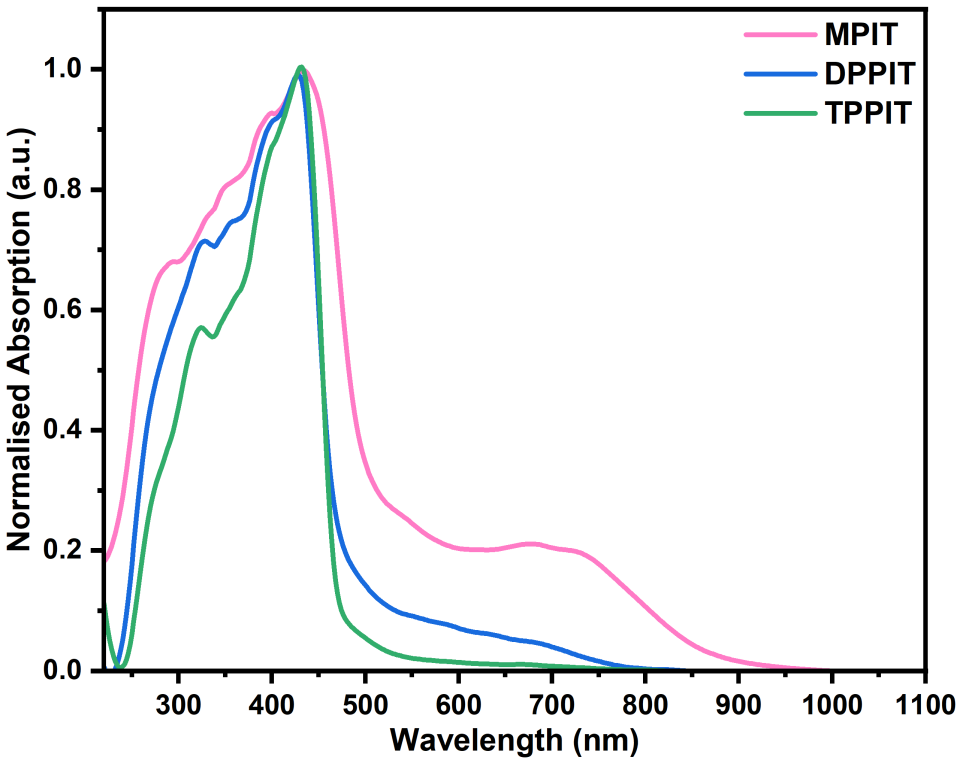

Figure S26: Diffused reflectance spectrum of **MPIT**, **DPPIT** and **TPPIT**.

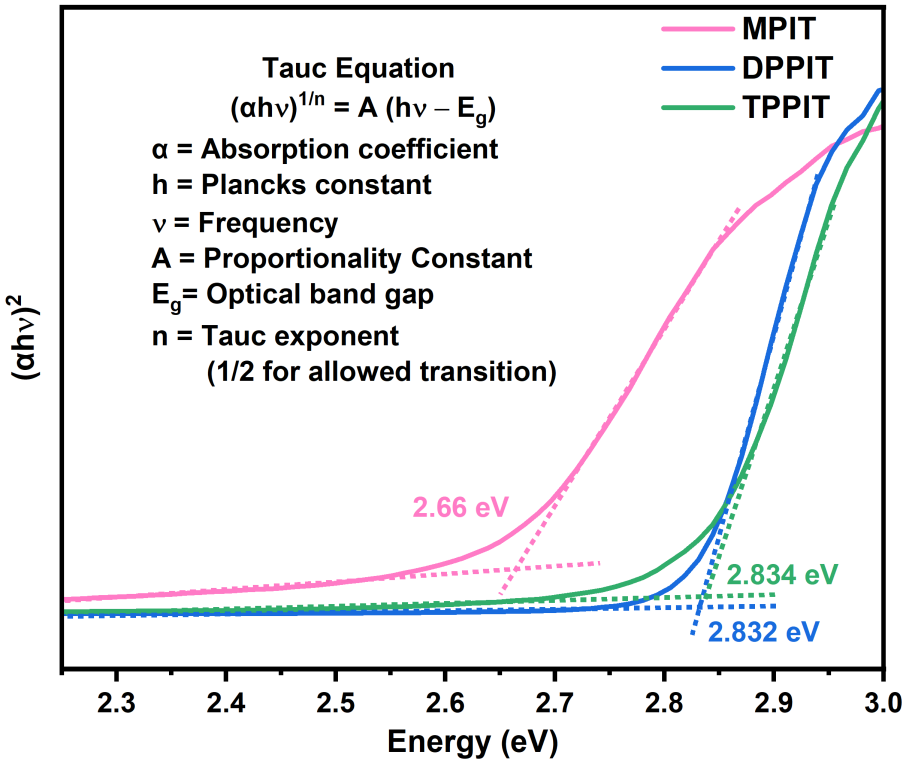

Figure S27: Tauc's plot for direct band gap energies of **MPIT**, **DPPIT** and **TPPIT**.

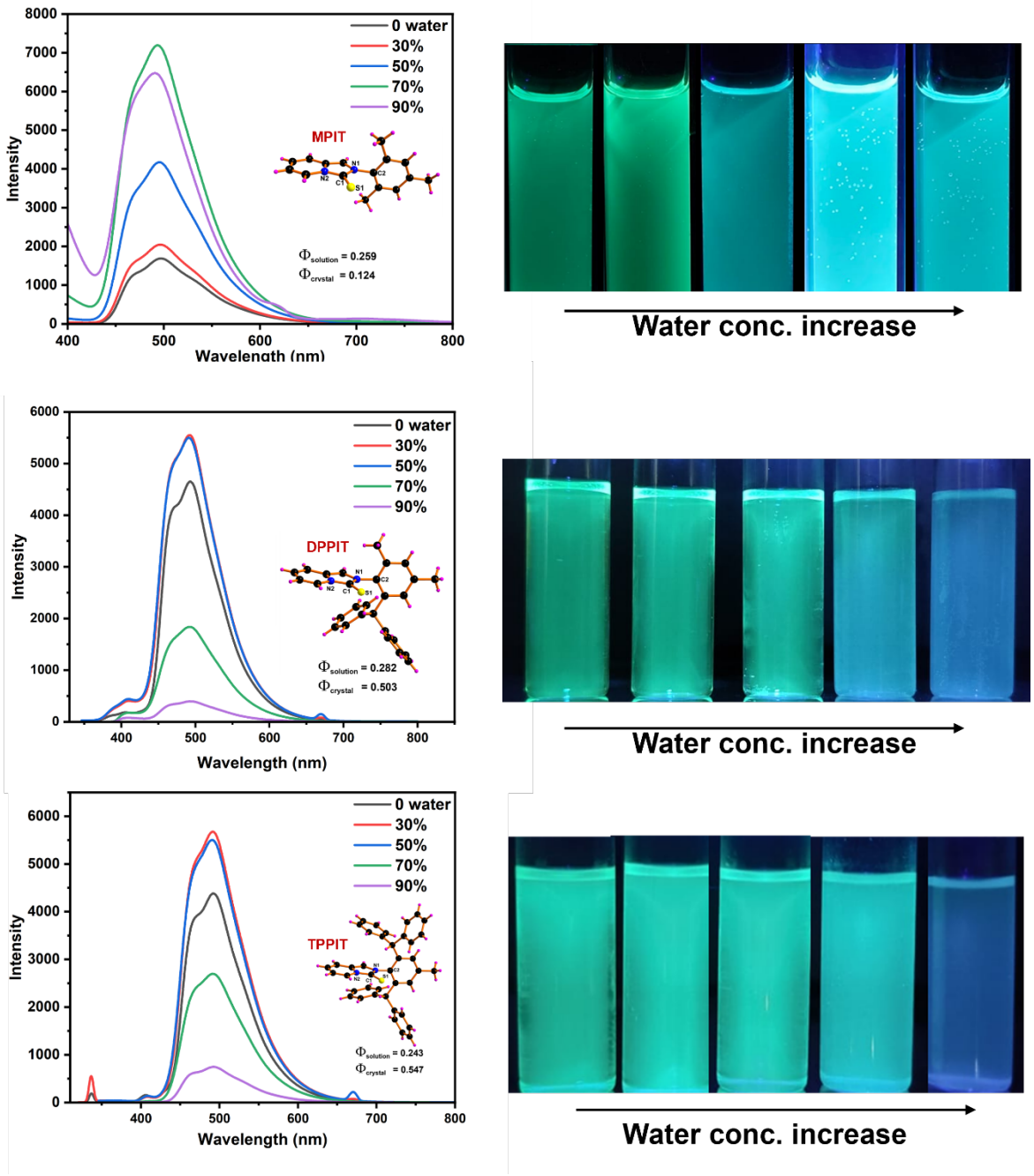

Figure S28: AIE test for **MPIT**, **DPPIT** and **TPPIT** in THF/Water.

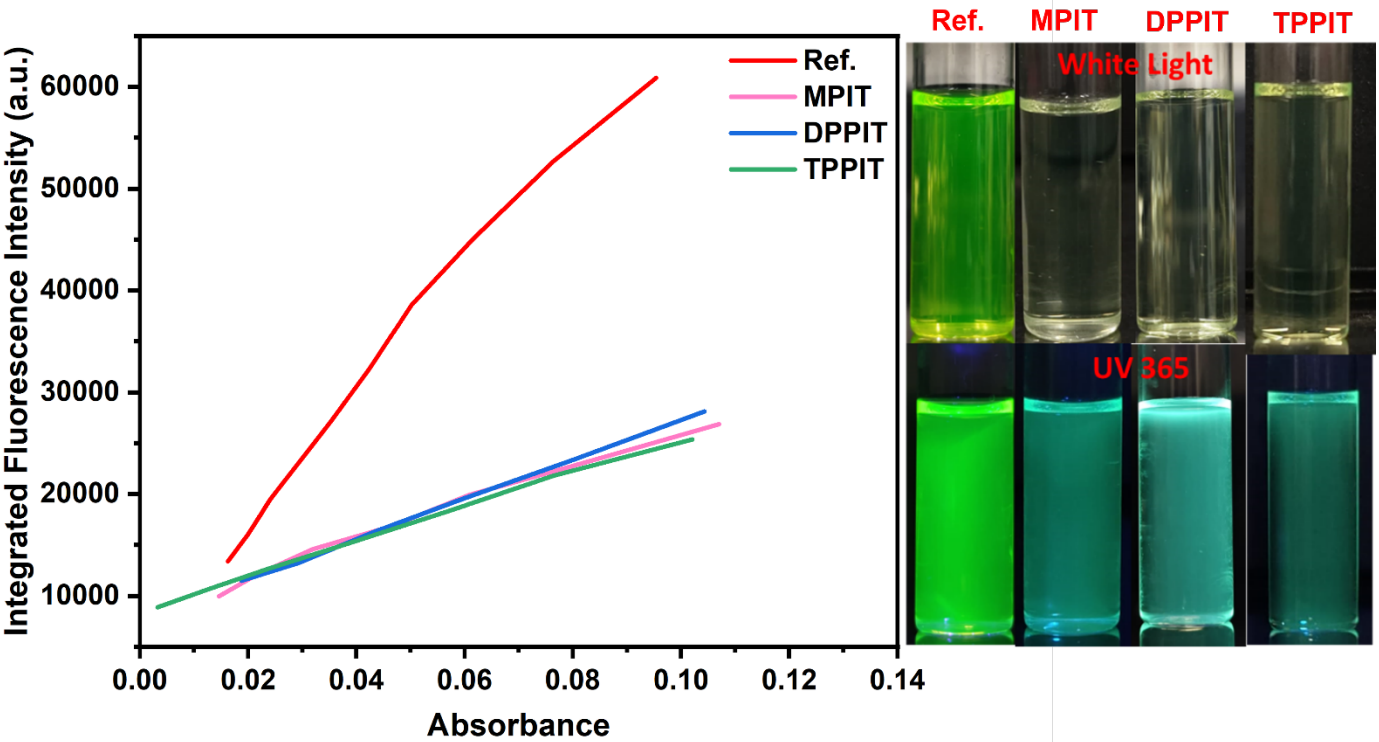

Figure S29: Integrated fluorescence intensity plot for relative Quantum yield using fluorescein (ϕ_f= 0.89) as reference.

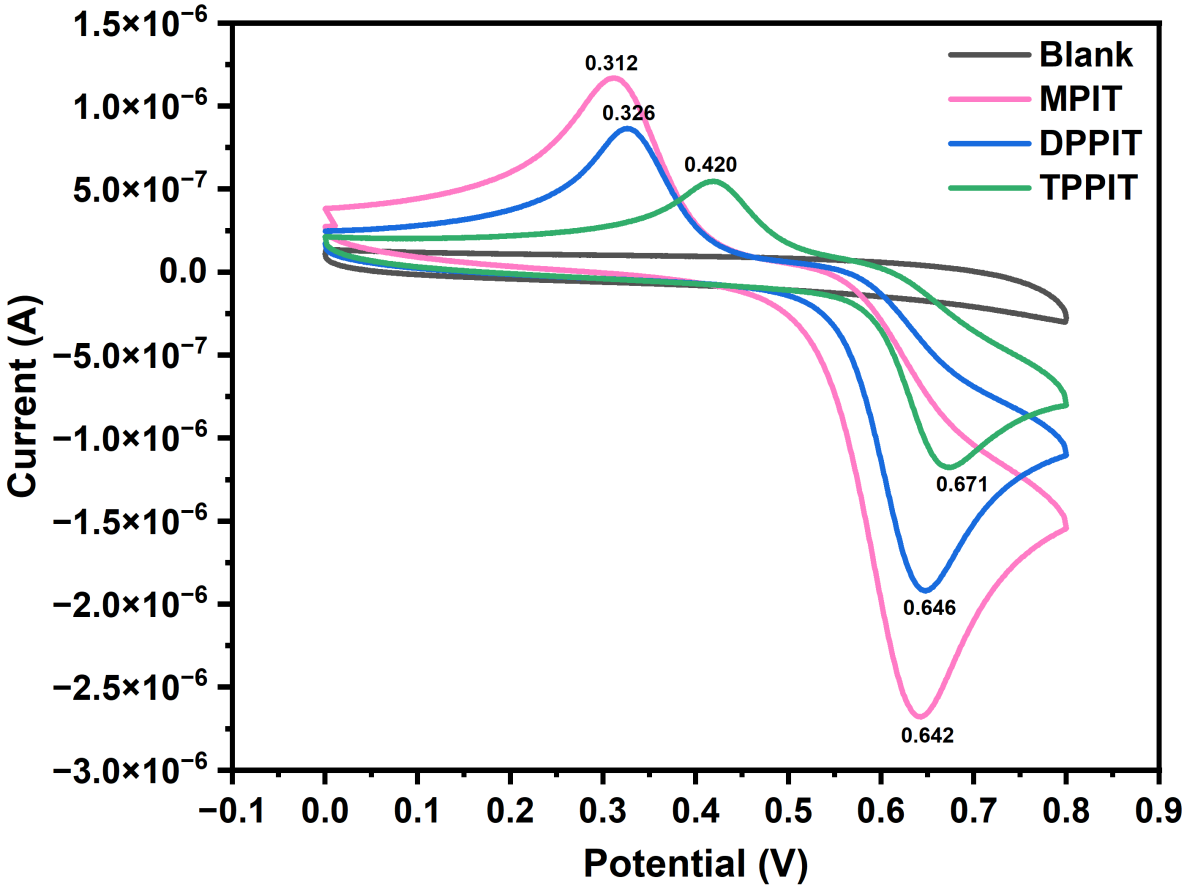

Figure S30: Cyclic voltammetry plot of **MPIT**, **DPPIT** and **TPPIT** (0.3 mM CH_3CN solution) using Ag/AgCl as reference electrode, platinum electrode as working and 0.1M $TBAClO_4$ as supporting electrolyte.

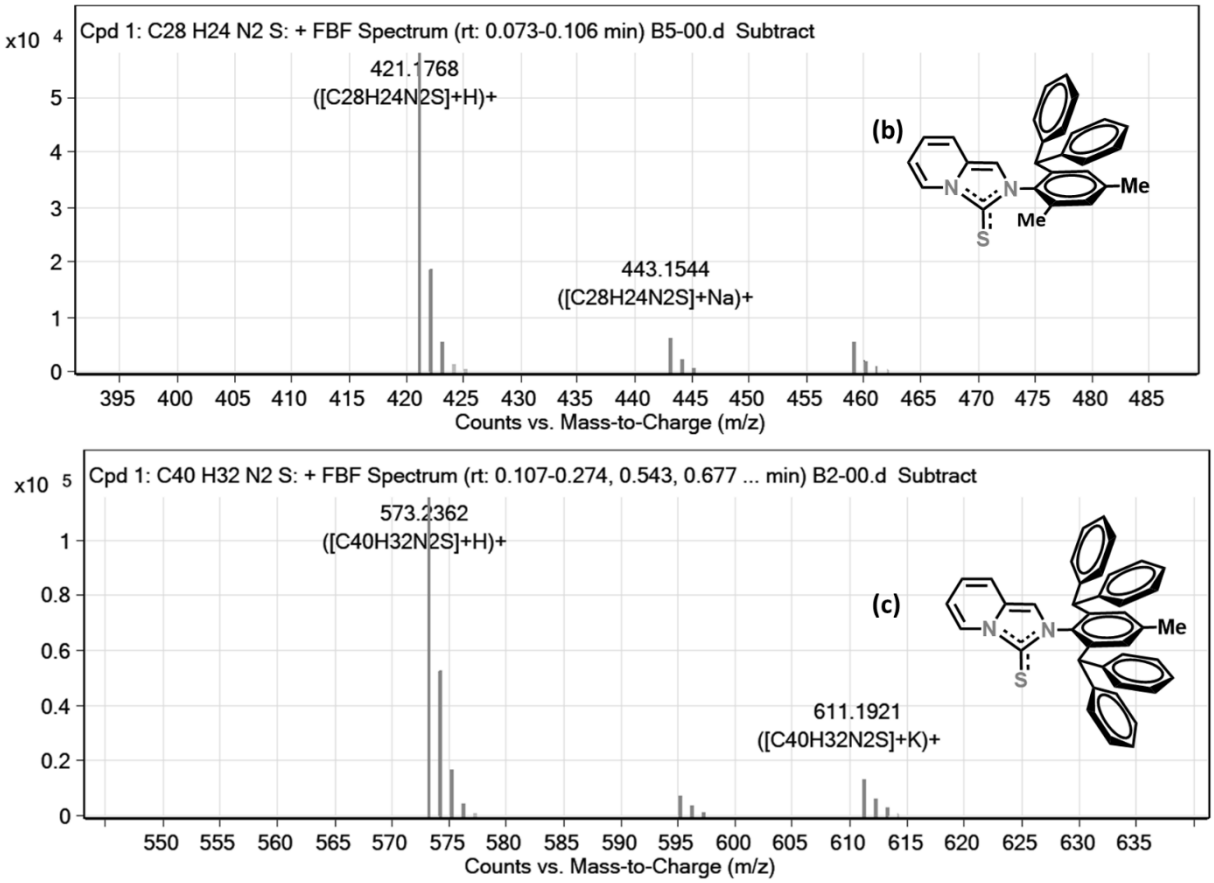

Figure S31: HRMS spectra for **DPPIT**(b) and **TPPIT**(c).

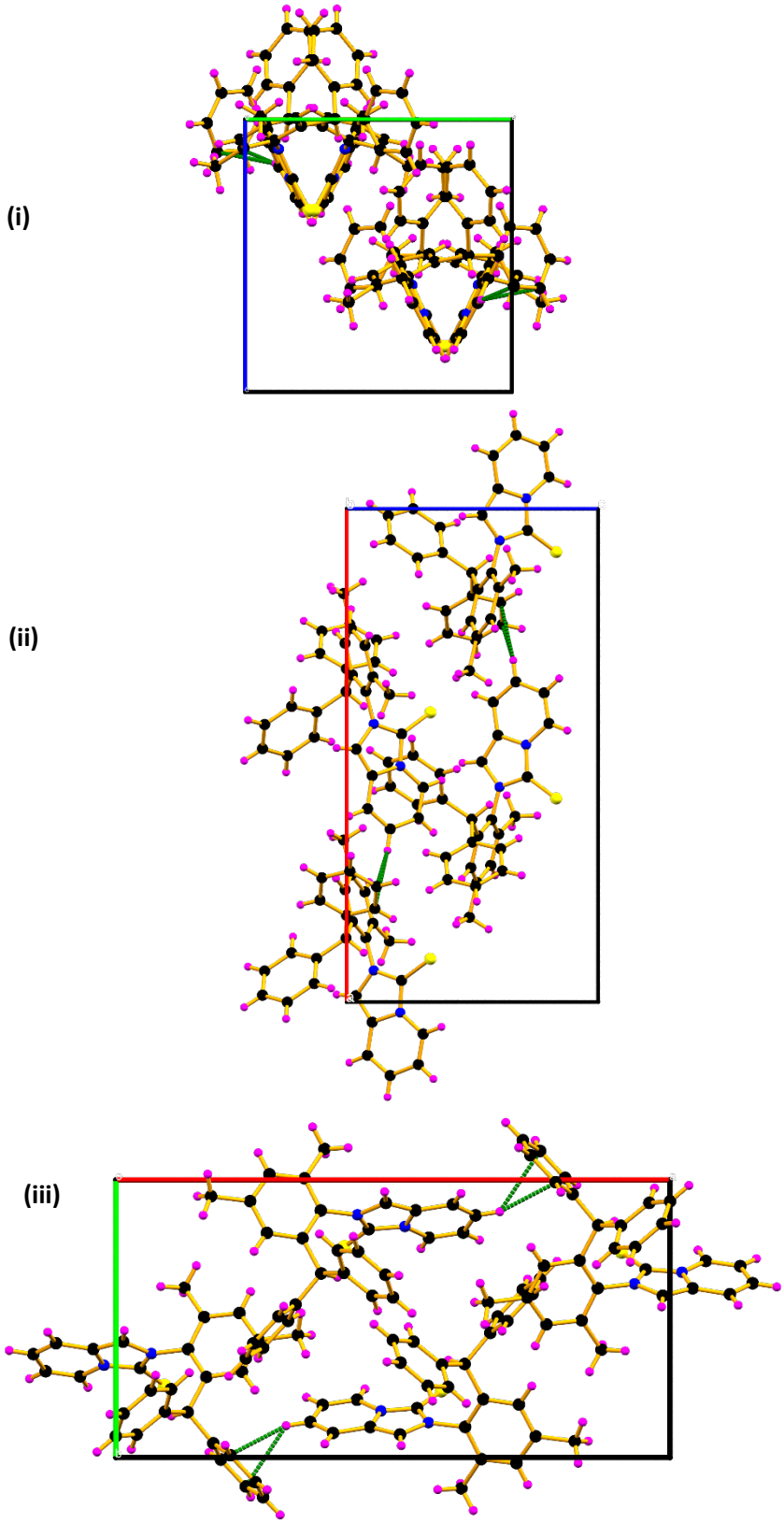

Figure S32: Molecular packing of **DPPIT** along a(i), b(ii) and c(iii) axis.

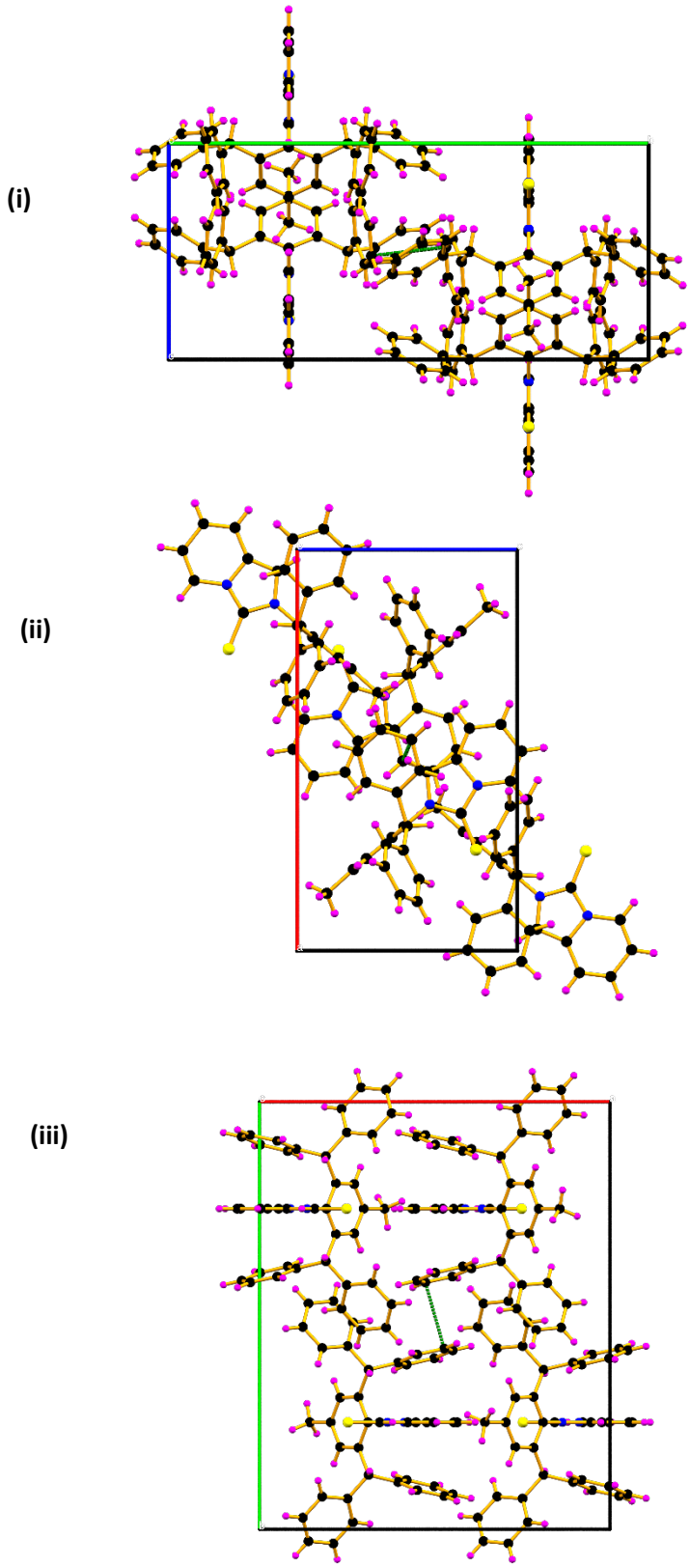

Figure S33: Molecular packing of **TPPIT** along a(i), b(ii) and c(iii) axis.

(i)

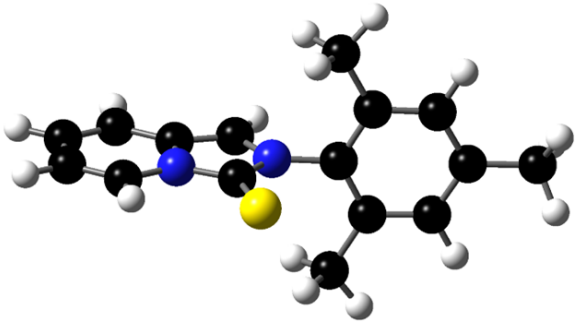

(ii)

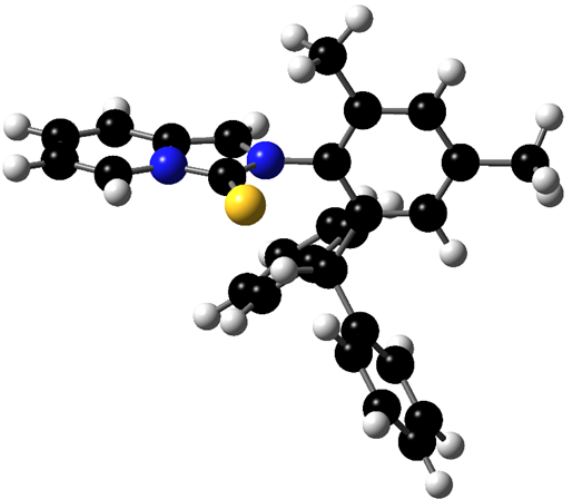

(iii)

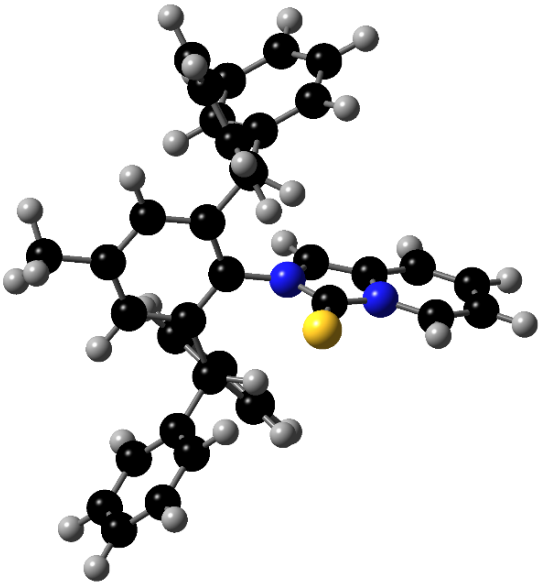

Figure S34: Optimized structures of **MPIT**(i), **DPPIT** (ii) and **TPPIT** (iii).

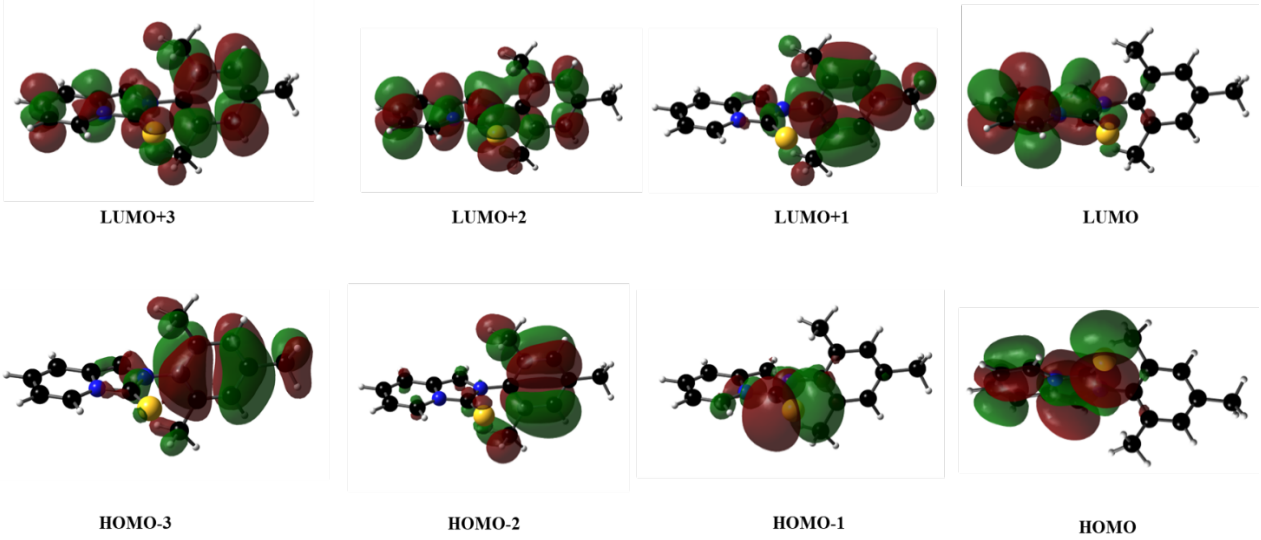

Figure S35: Frontier molecular orbitals of **MPIT**.

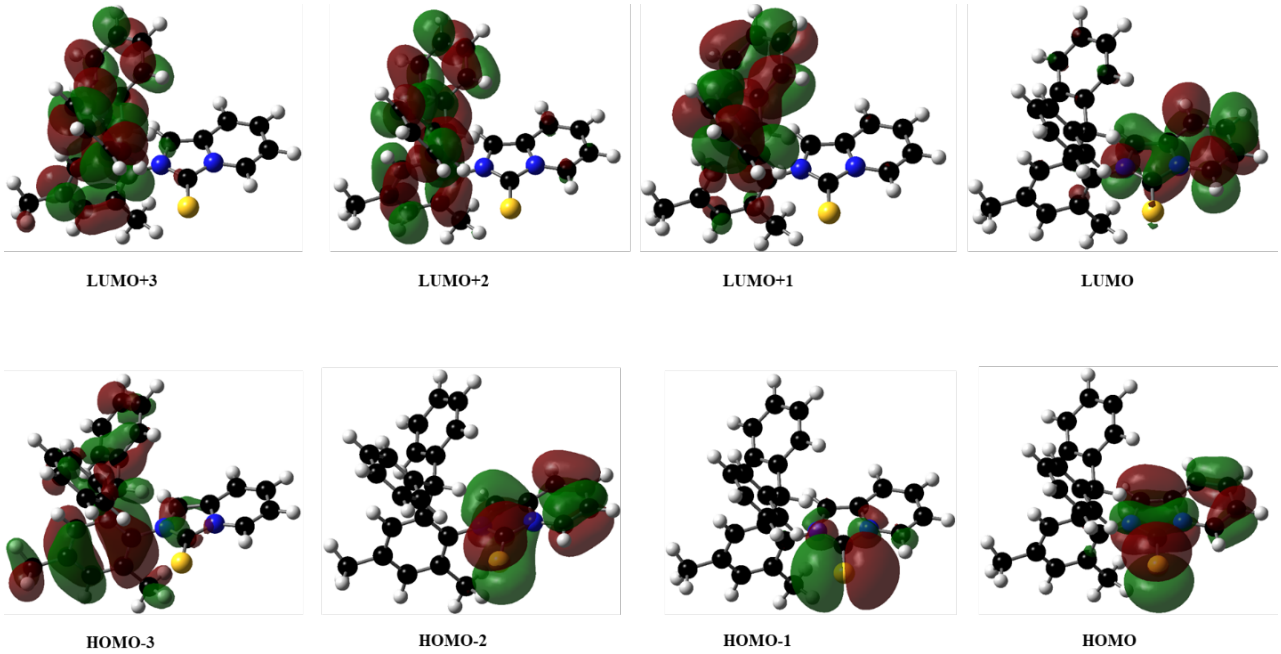

Figure S36: Frontier molecular orbitals of **DPPIT**.

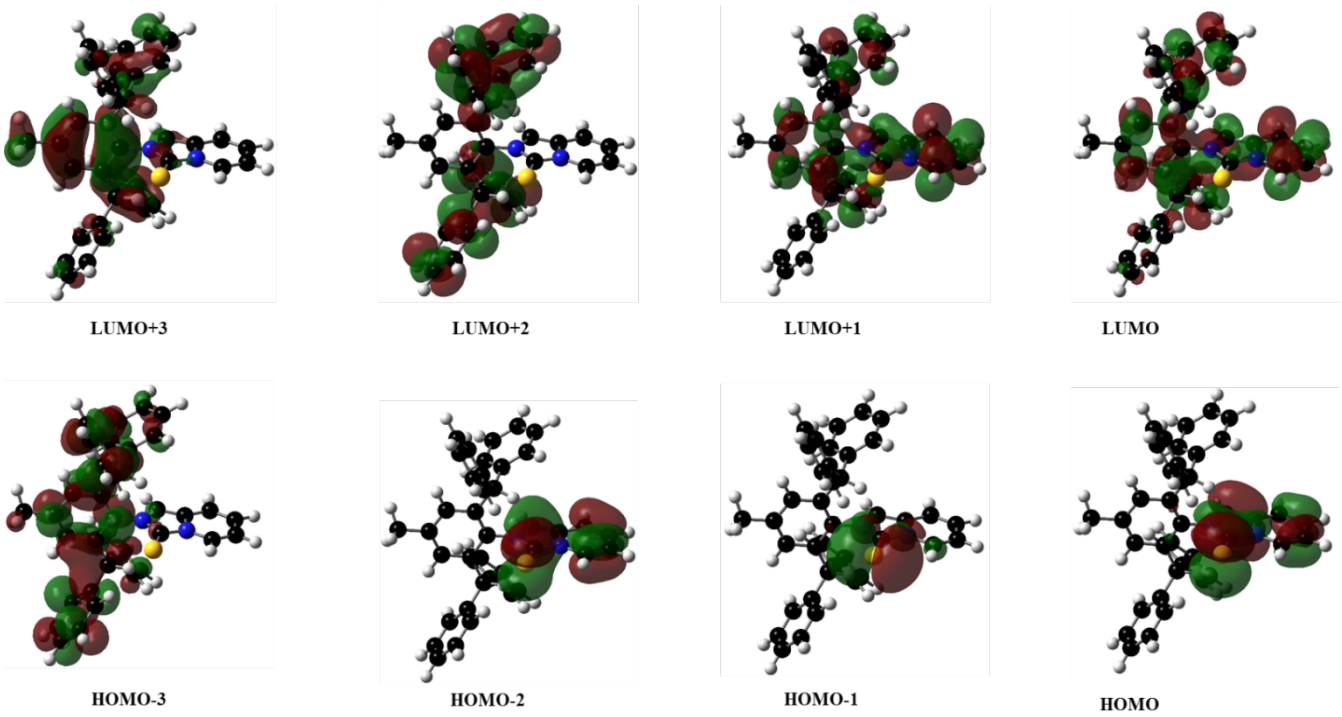

Figure S37: Frontier molecular orbitals of **TPPIT**

.

(a)

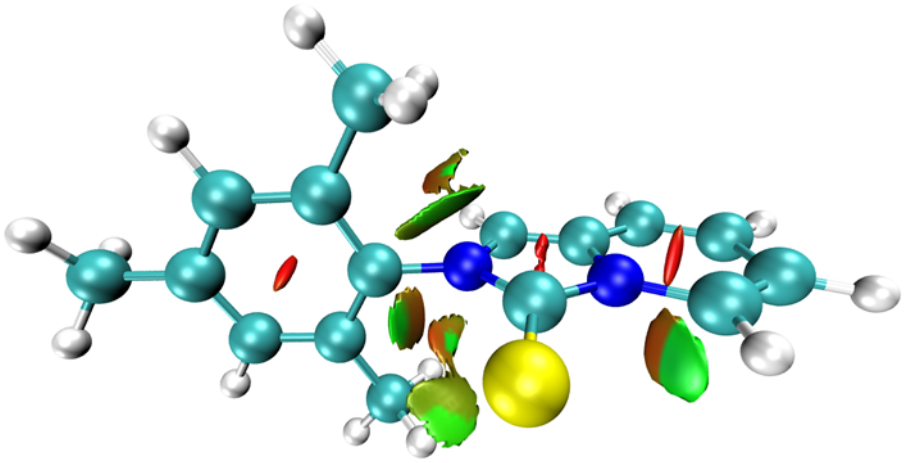

(b)

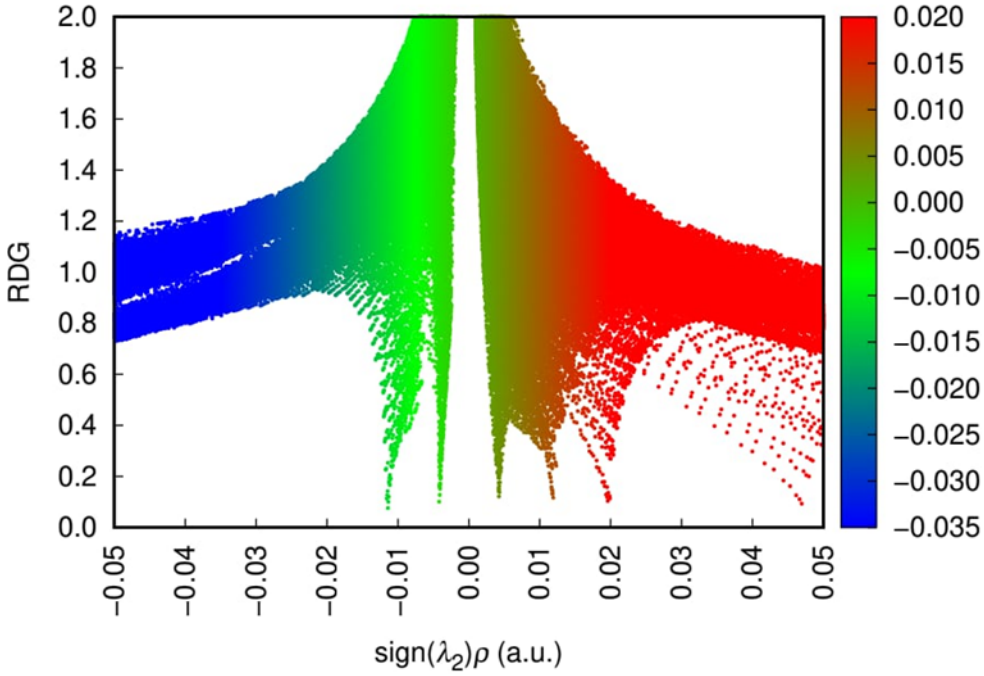

Figure S38: Visualization of (a) intramolecular contacts in **MPIT** using NCI analysis with blue-green-red scheme over the -0.05 < sign(λ_2)ρ < 0.05 a.u in 3D. Here, ρ means the density of the electron, and sign (λ_2) is the sign of the second largest eigenvalue of the Hessian matrix of ρ. The interaction between sulfur and hydrogen in green color suggests van der Waals interactions. (b) The scatter graph plot of RDG vs. sign(λ_2)ρ is also depicted along with the isosurface plot.

(a)

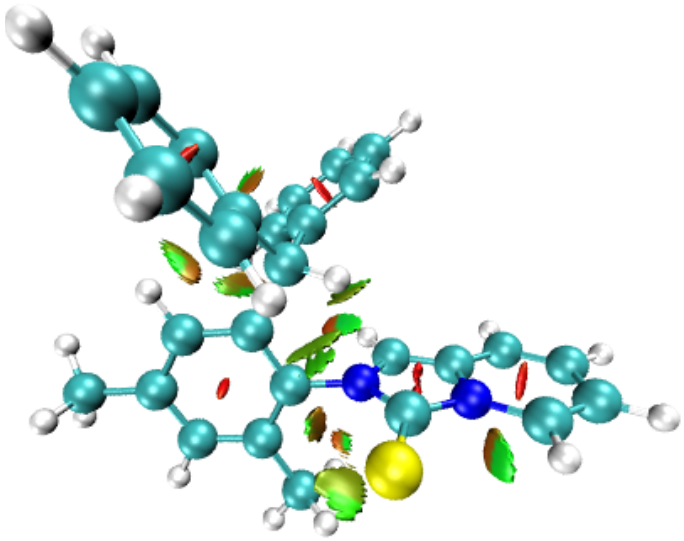

(b)

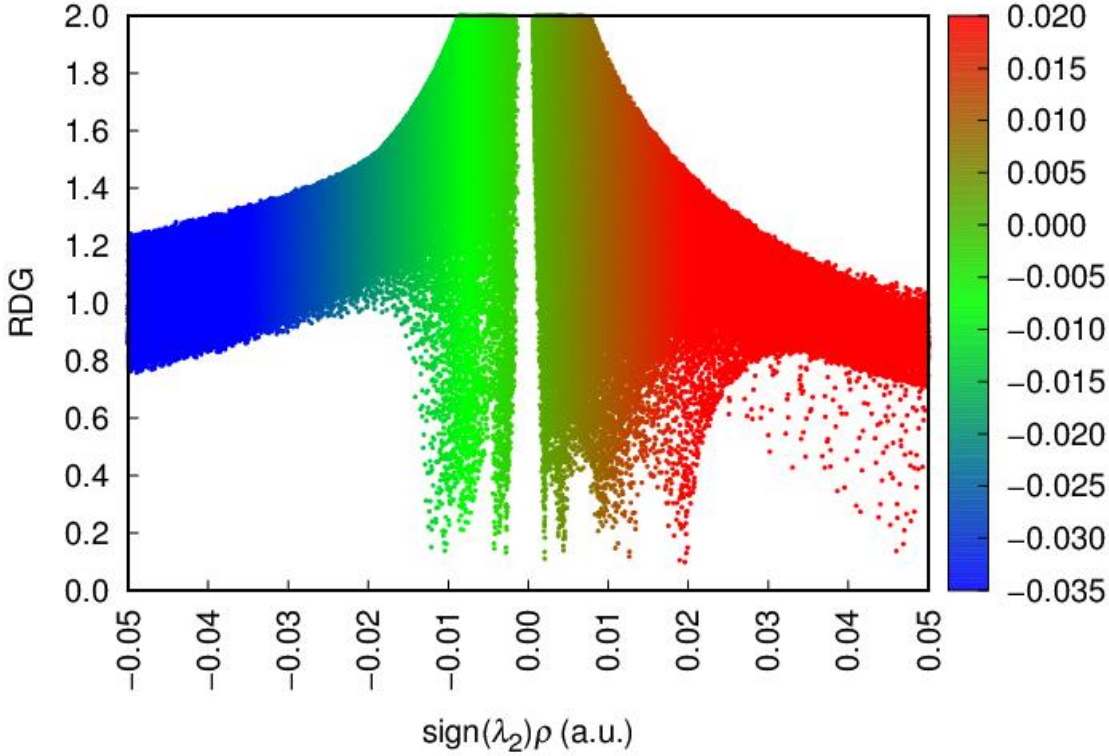

Figure S39: Visualization of (a) intramolecular contacts in **DPPIT** using NCI analysis with blue-green-red scheme over the -0.05 < sign(λ_2)ρ < 0.05 a.u in 3D. Here, ρ means the density of the electron, and sign (λ_2) is the sign of the second largest eigenvalue of the Hessian matrix of ρ. The interaction between sulfur and hydrogen in green color suggests van der Waals interactions. (b) The scatter graph plot of RDG vs. sign(λ_2)ρ is also depicted along with the isosurface plot.

(a)

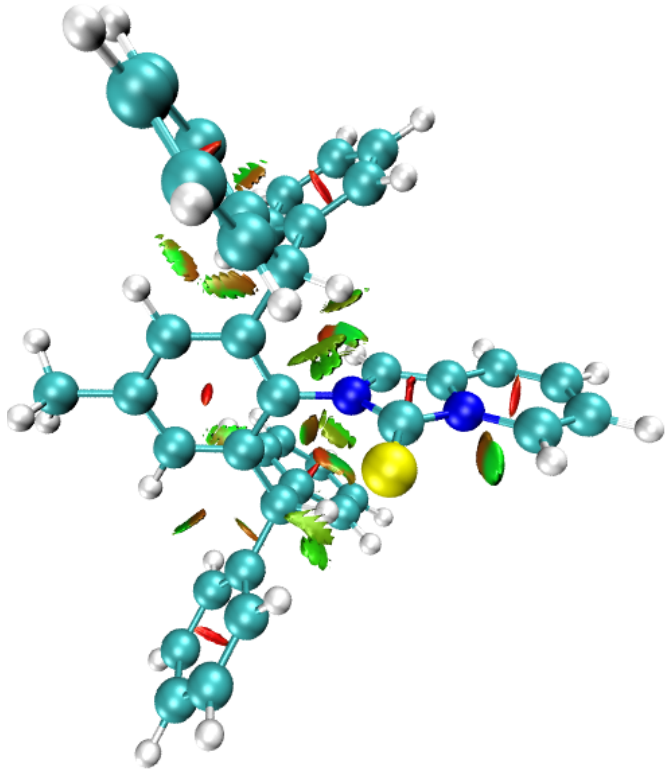

(b)

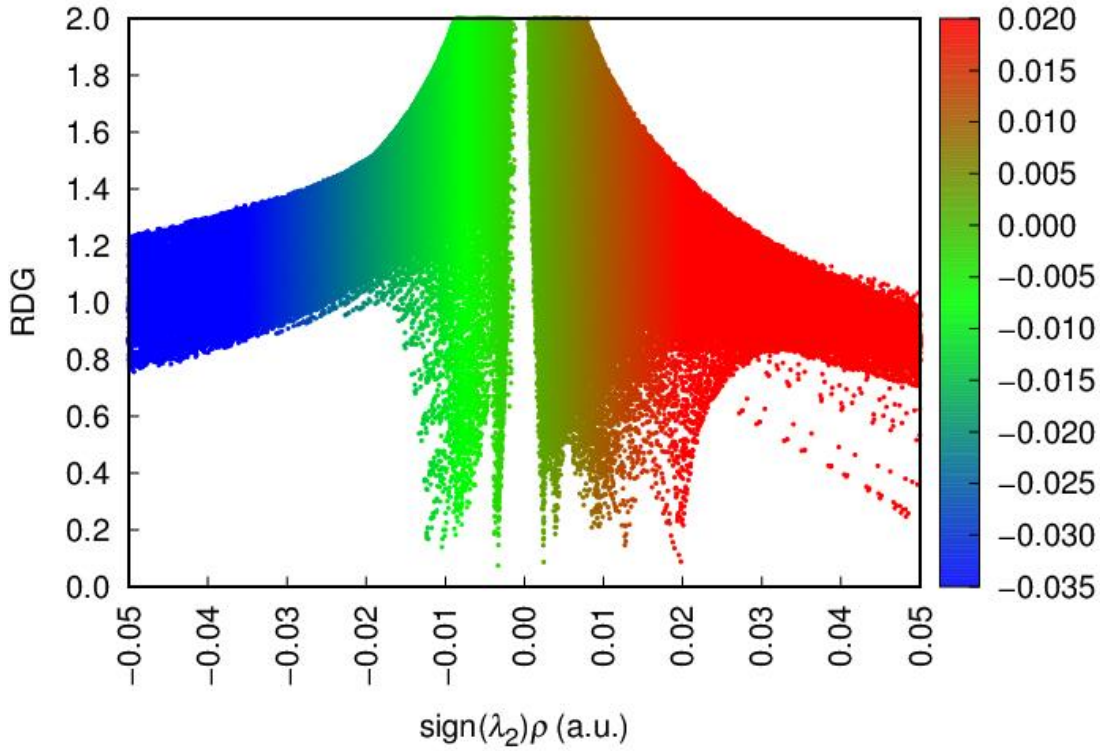

Figure S40: Visualization of (a) intramolecular contacts in **TPPIT** using NCI analysis with blue-green-red scheme over the -0.05 < sign(λ_2)ρ < 0.05 a.u in 3D. Here, ρ means the density of the electron, and sign (λ_2) is the sign of the second largest eigenvalue of the Hessian matrix of ρ. The interaction between sulfur and hydrogen in green color suggests van der Waals interactions. (b) The scatter graph plot of RDG vs. sign(λ_2)ρ is also depicted along with the isosurface plot.

(a)

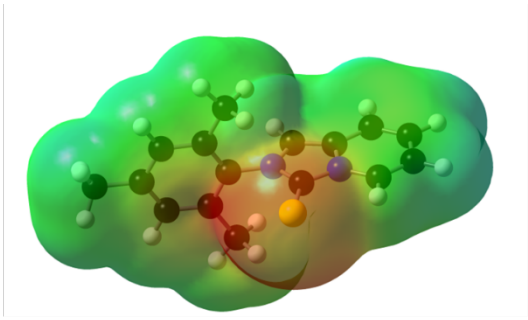

(b)

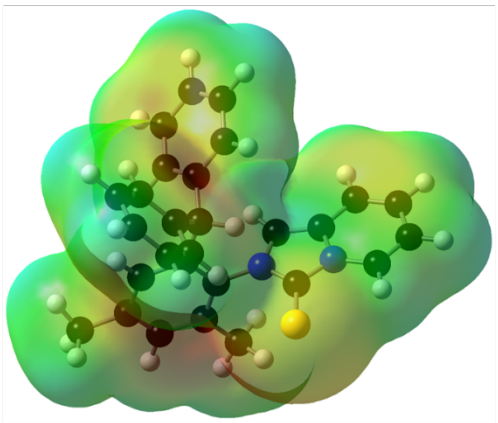

(c)

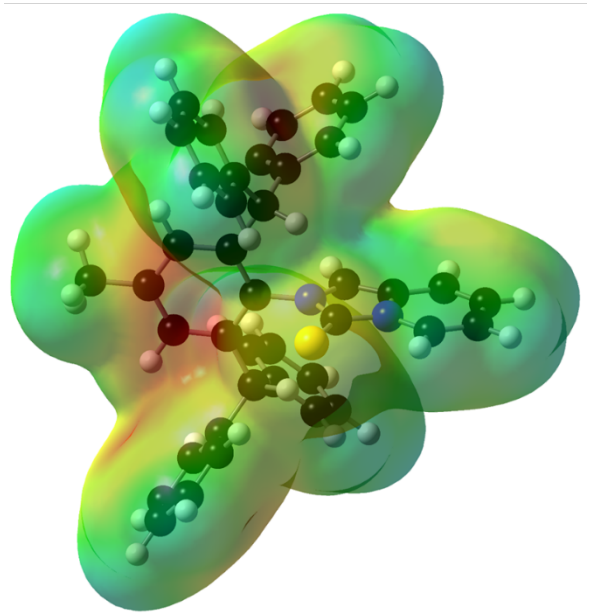

Figure S41: Ground state electron cloud of **MPIT**(a), **DPPIT**(b) and **TPPIT**(c).

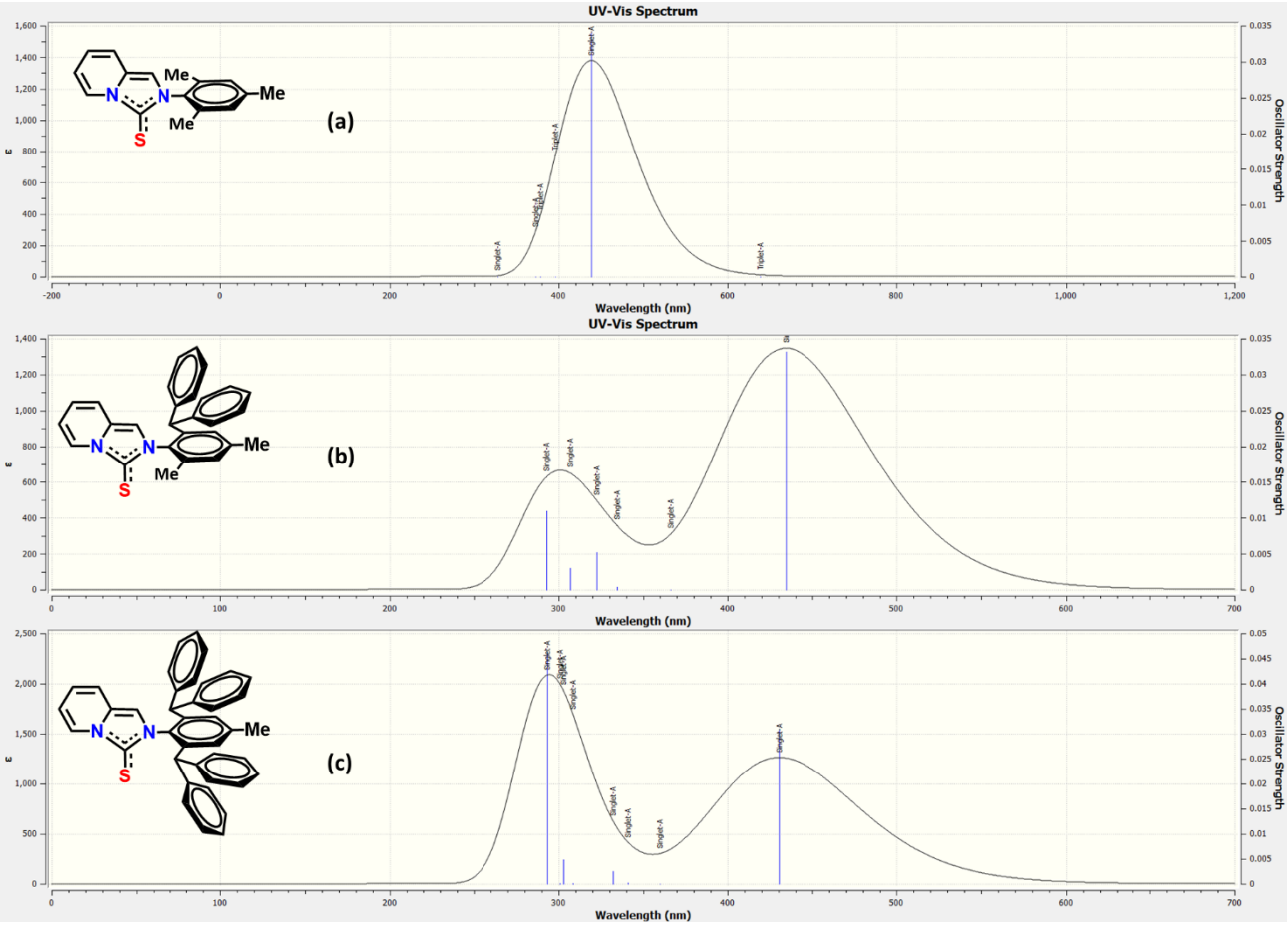

Figure S42: Calculated UV-Vis spectra of **MPIT**(i), **DPPIT**(ii) and **TPPIT**(iii) by TD-DFT.

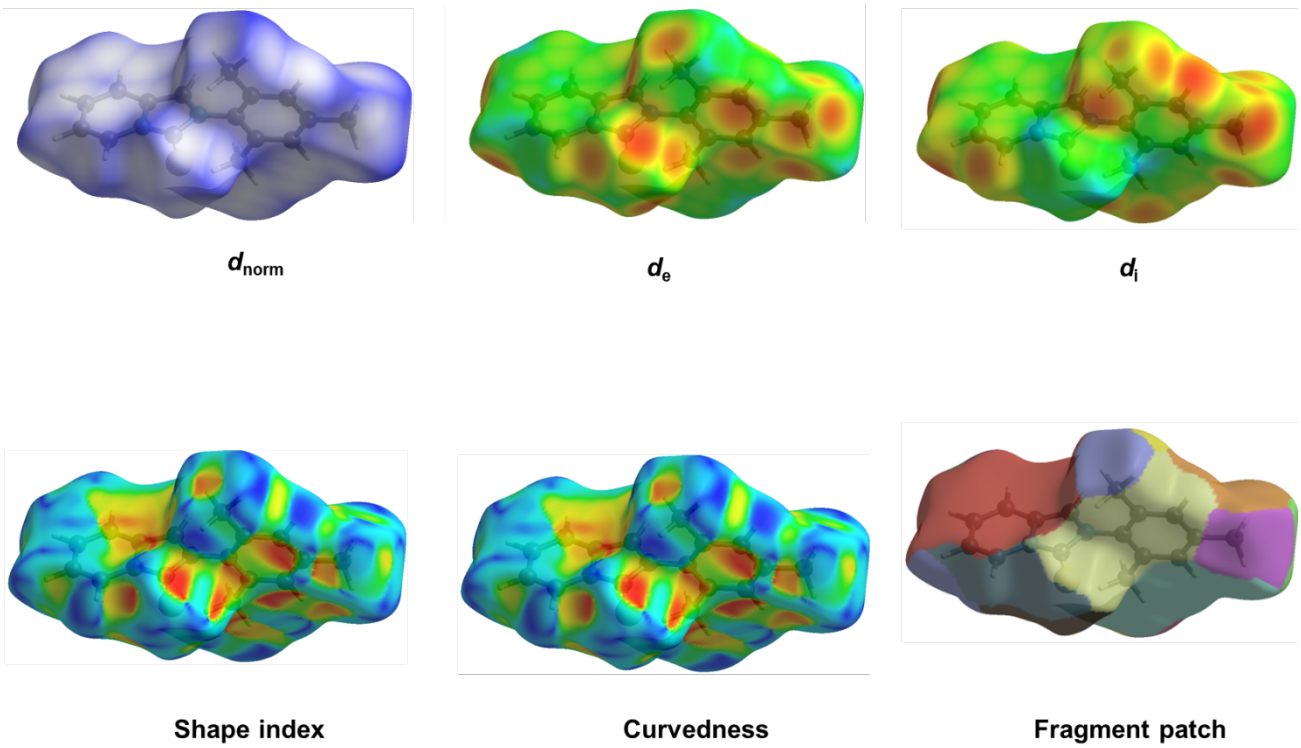

Figure S43: Hirshfeld surface mapping of **MPIT** shows various representations of non-covalent interactions.

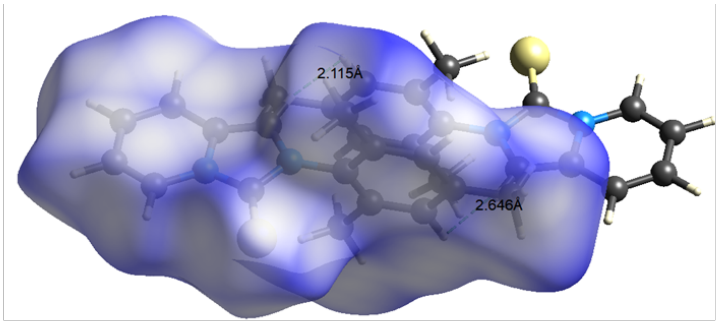

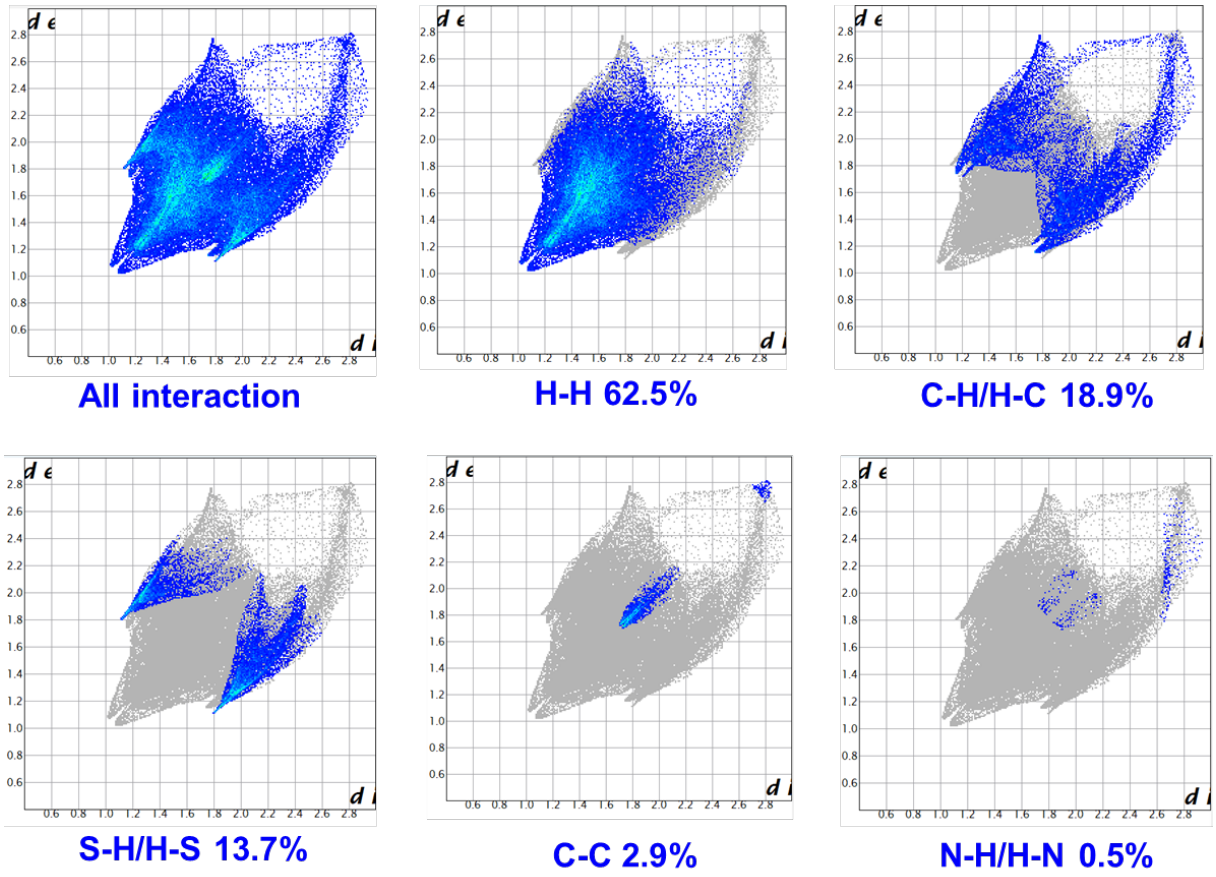

Figure S44: Hirshfeld surface interaction and fingerprint plots of **MPIT** show various kinds of non-covalent interactions.

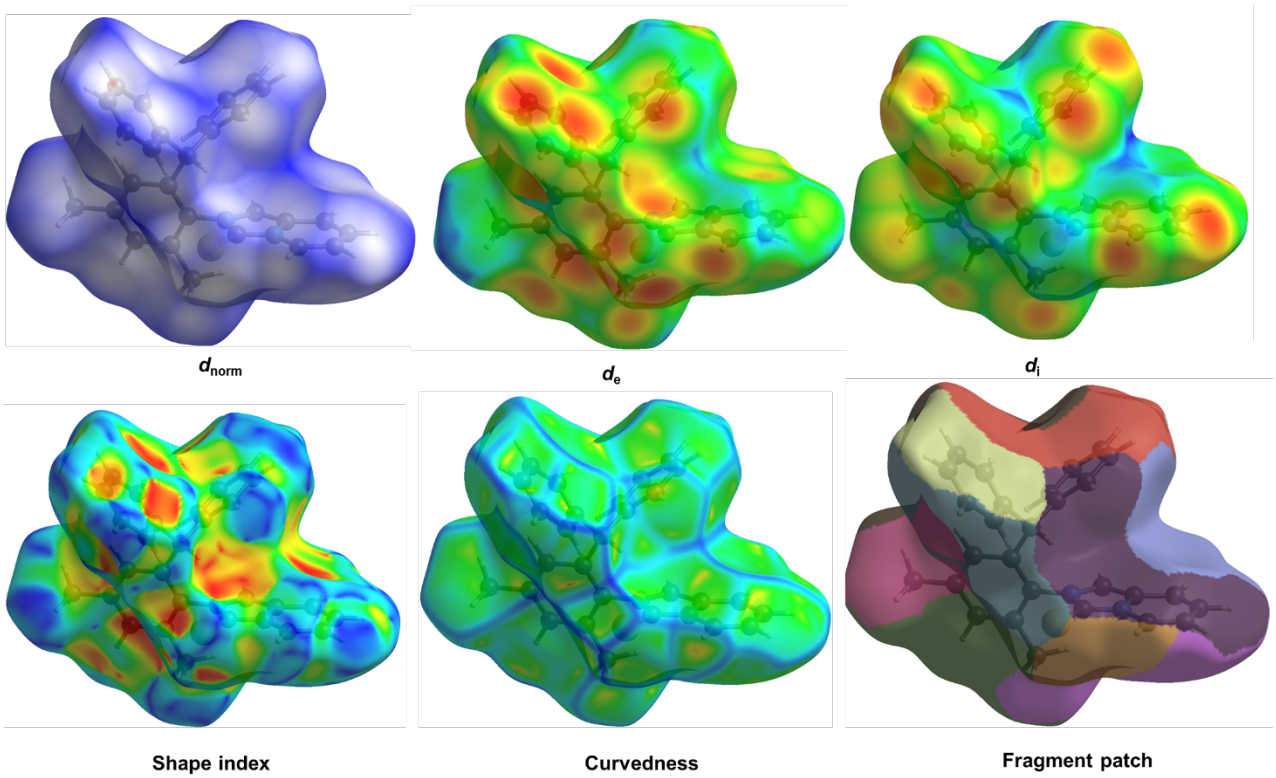

Figure S45: Hirshfeld surface mapping of **DPPIT** shows various representations of non-covalent interactions

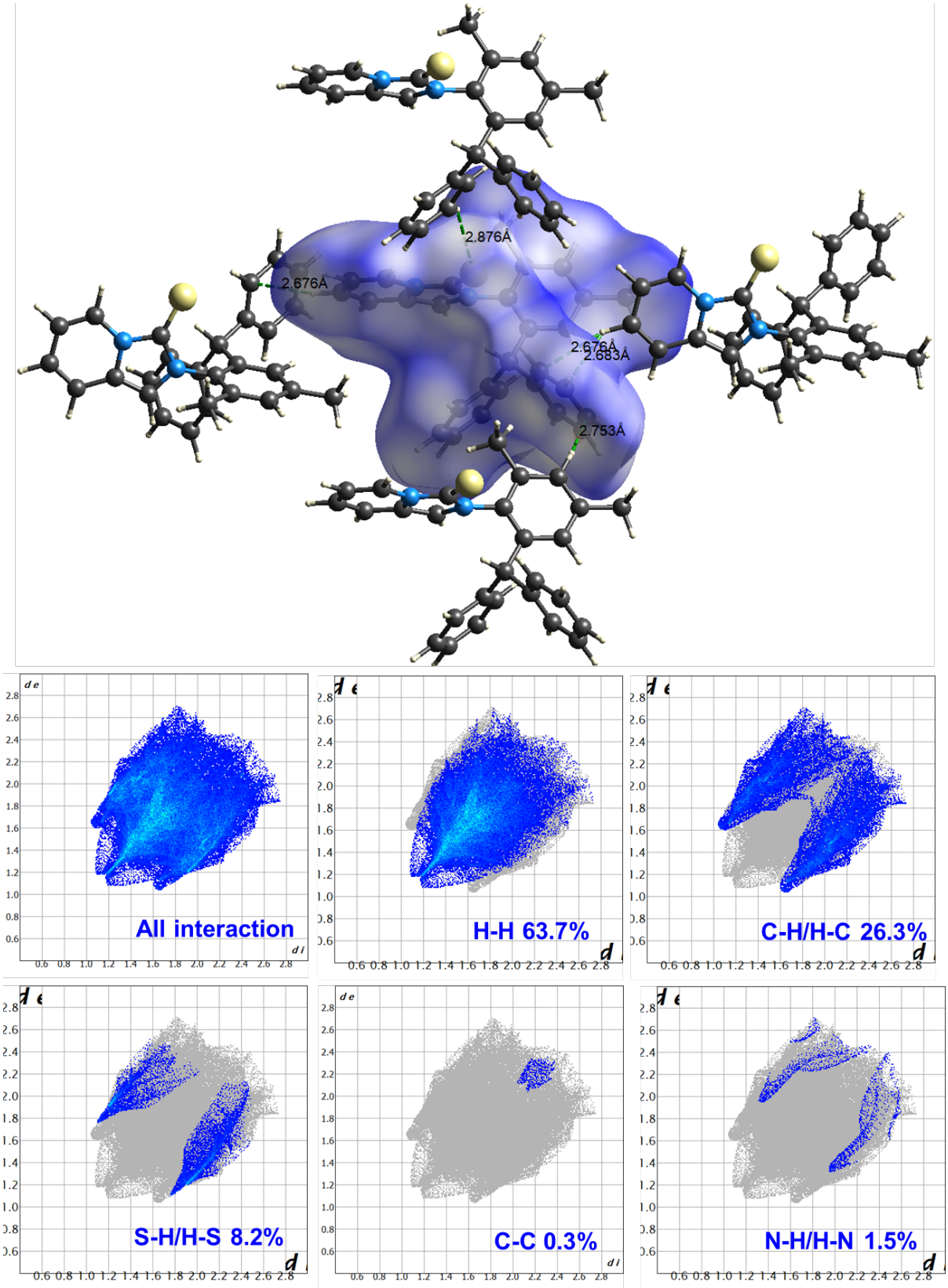

Figure S46: Hirshfeld surface interaction and fingerprint plots of **DPPIT** show various kinds of non-covalent interactions.

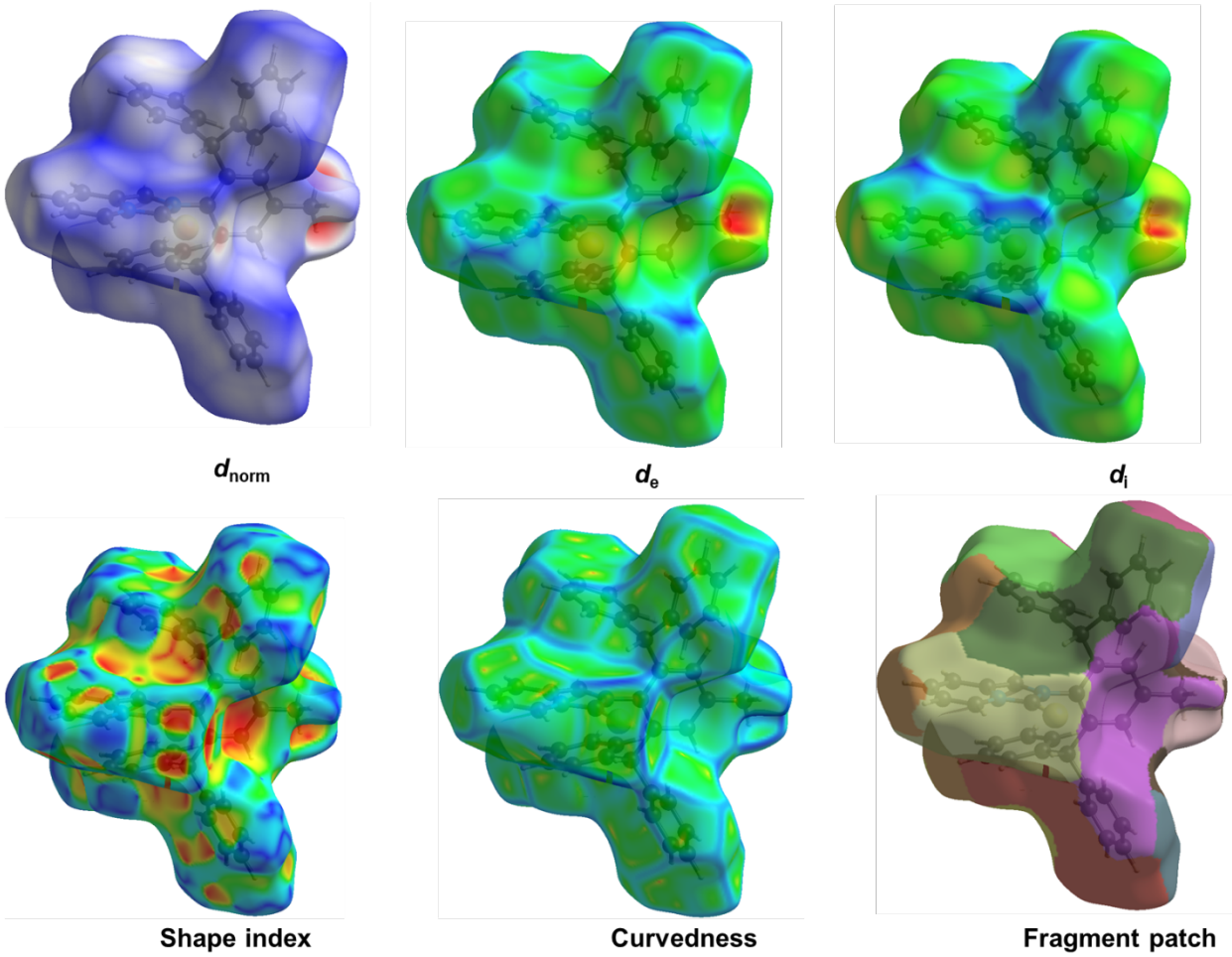

Figure S47: Hirshfeld surface mapping of **TPPIT** shows various representations of non-covalent interactions.

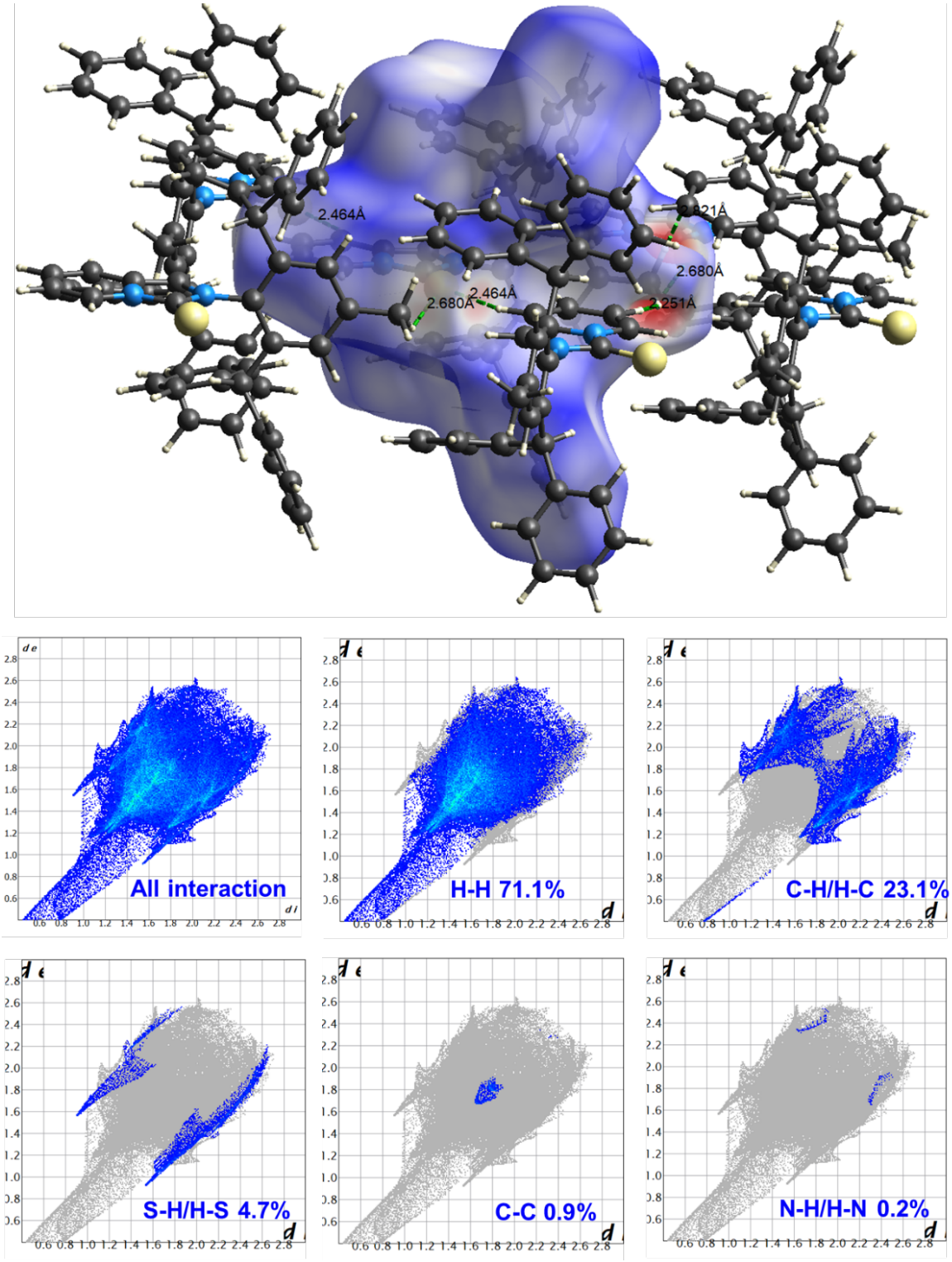

Figure S48: Hirshfeld surface interaction and fingerprint plots of **TPPIT** show various kinds of non-covalent interactions.

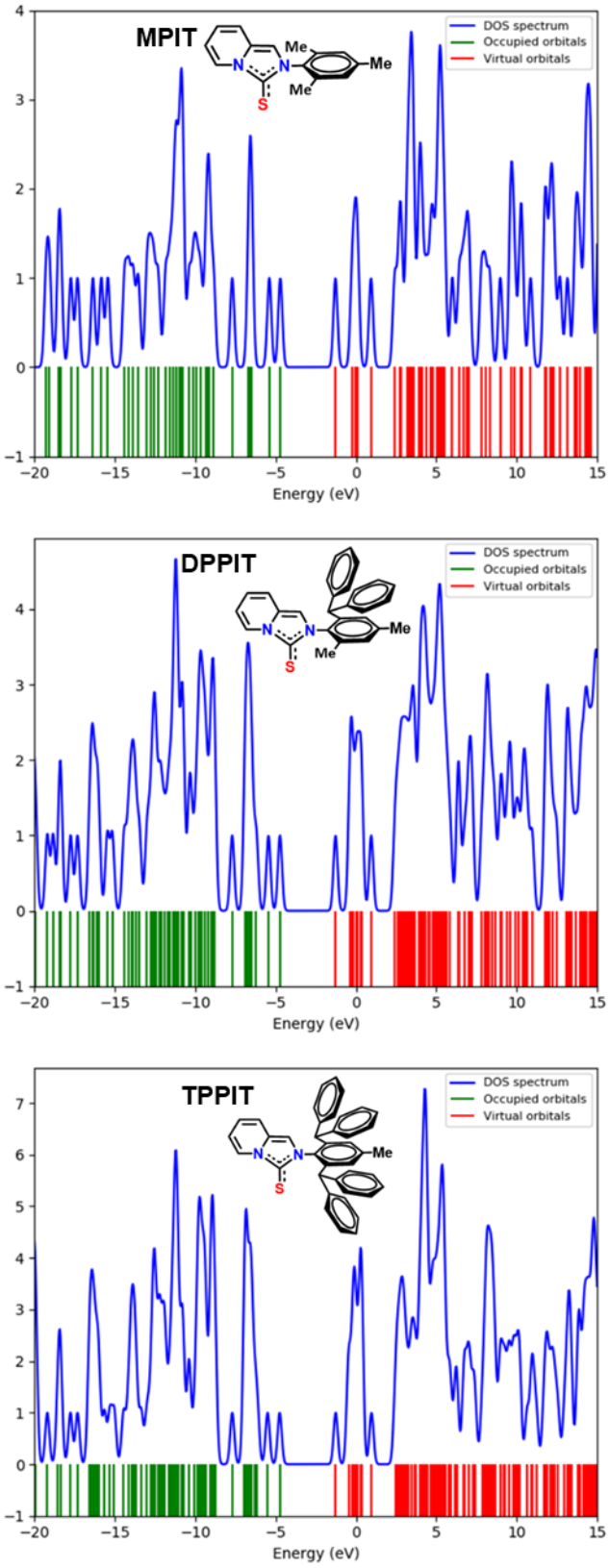

Figure S49: DOS spectra of **MPIT**, **DPPIT** and **TPPIT** using TD-DFT calculation in the range of -20 to 15 eV.

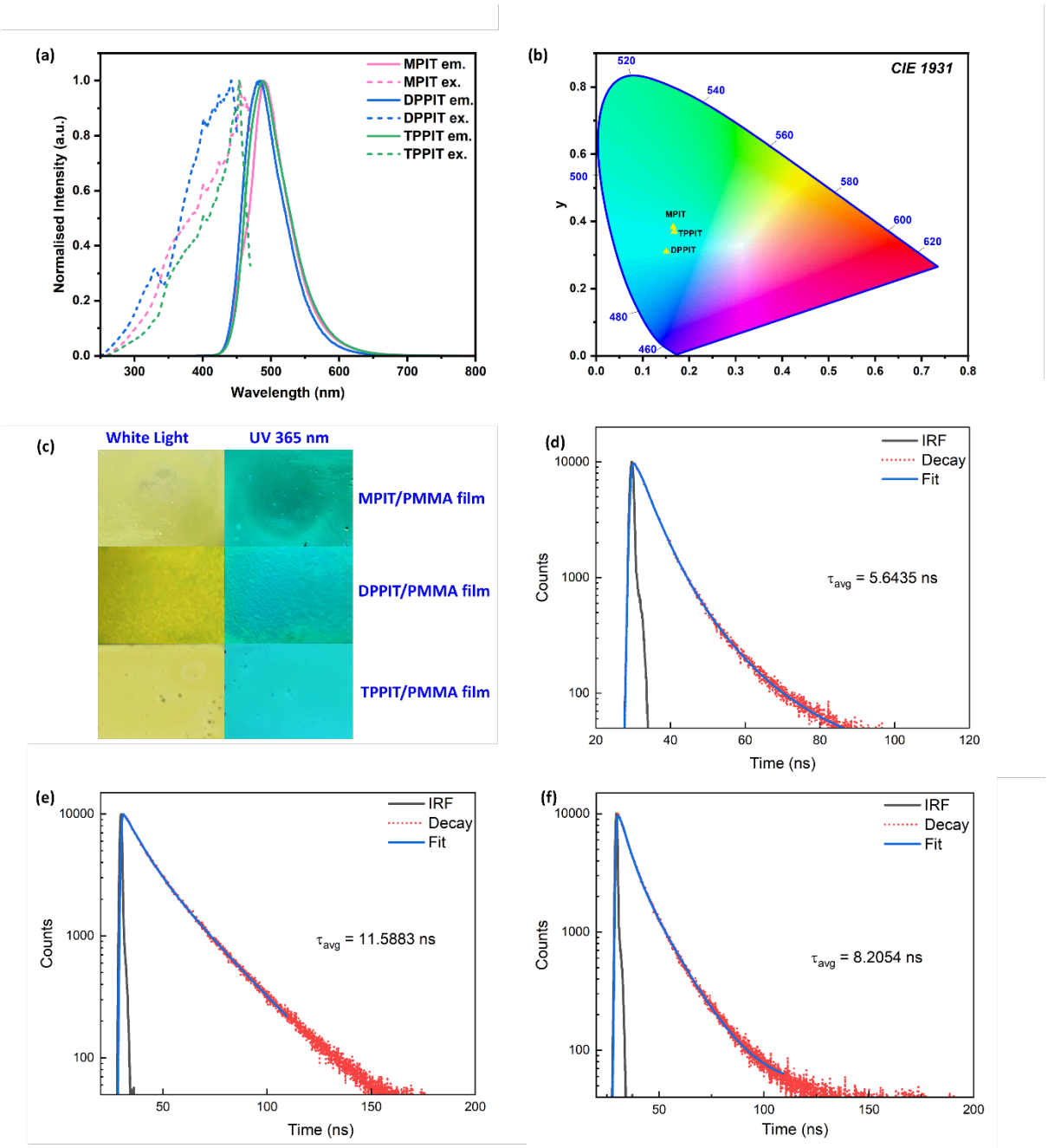

Figure S50: Photoluminescence properties of solid film **MPIT**, **DPPIT** and **TPPIT**, (a) Emission-Excitation spectra of films, (b) CIE diagram, (c) snaps of films under ambient and UV light and Lifetime decay for **MPIT** (d), **DPPIT** (e) and **TPPIT** (f).

Table S1: Structural parameters for **DPPIT** and **TPPIT**.

	DPPIT	**TPPIT**
Empirical formula	$C_{28}H_{24}N_2S$	$C_{40}H_{32}N_2S$
Formula weight	420.55	572.73
Temperature/K	298	298
Crystal system	orthorhombic	orthorhombic
Space group	*Pna*2_1	*Pnma*
a/Å	20.9290(16)	16.8230(16)
b/Å	10.4742(8)	20.529(3)
c/Å	10.6843(8)	9.2298(11)
α/°	90	90
β/°	90	90
γ/°	90	90
Volume/Å^3	2342.2(3)	3187.6(6)
Z	4	4
ρ_{calc}g/cm^3	1.193	1.194
μ/mm-1	0.155	0.132
F(000)	888.9	1209.1
Crystal size/mm^3	0.27 × 0.21 × 0.17	0.26 × 0.13 × 0.05
Radiation	MoK$_\alpha$ (λ = 0.71073)	MoK$_\alpha$ (λ = 0.71073)
2Θ range for data collection/°	3.9 to 54.78	4.84 to 54.28
Index ranges	$-26 \leq h \leq 26$, $-13 \leq k \leq 13$, $-13 \leq l \leq 13$	$-20 \leq h \leq 21$, $-26 \leq k \leq 25$, $-11 \leq l \leq 11$
Reflections collected	66460	26722
Independent reflections	5213 [R_{int} = 0.1111, R_{sigma} = 0.0568]	3609 [R_{int} = 0.1056, R_{sigma} = 0.0650]
Data/restraints/parameters	5213/1/282	3608/0/230
Goodness-of-fit on F_2	1.038	1.64
Final R indexes [I>=2σ (I)]	R_1 = 0.0476, wR_2 = 0.1150	R_1 = 0.0622, wR_2 = 0.1352
Final R indexes [all data]	R_1 = 0.1017, wR_2 = 0.1483	R_1 = 0.1036, wR_2 = 0.1582
Largest diff. peak/hole / e Å^{-3}	0.20/-0.29	0.27/-0.29

Table S2: Selected bond parameters for **DPPIT** and **TPPIT**.

Selected bond angles

S.no	Atom	Atom	Atom	**DPPIT** (°)	**TPPIT** (°)
1.	N1	C1	S1	128.4(2)	128.0(2)
2.	N2	C1	S1	127.4(2)	127.3(2)
3.	N2	C1	N1	104.2(2)	104.7(2)
4.	C1	N1	C2	123.2(2)	123.6(2)

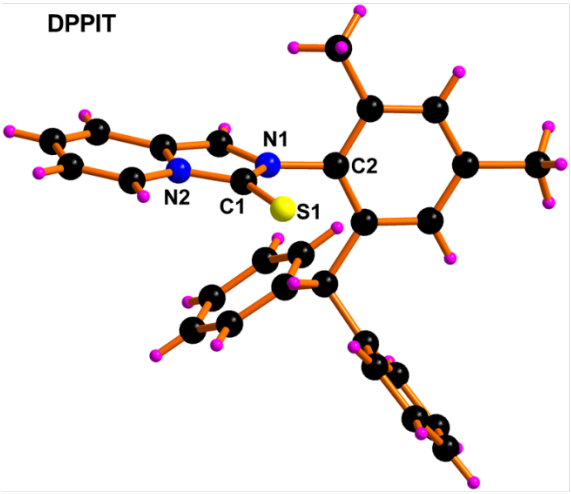

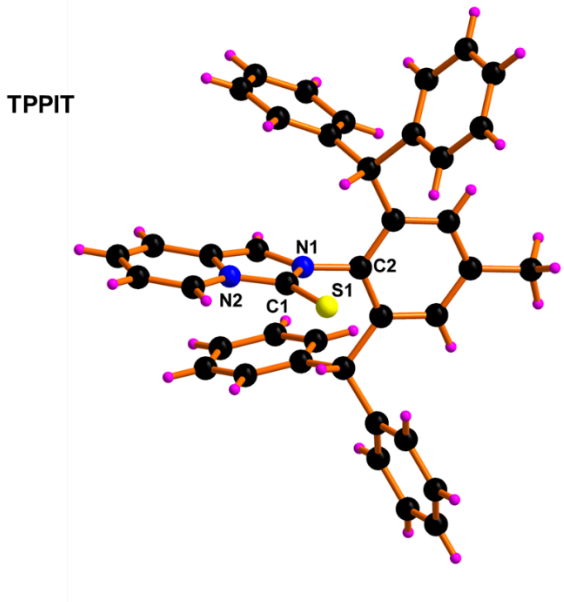

Selected bond distance

S.no.	Atom	Atom	**DPPIT** (Å)	**TPPIT** (Å)
1.	S1	C1	1.666(3)	1.650(3)
2.	N1	C2	1.438(3)	1.438(3)
3.	N1	C1	1.368(3)	1.358(4)
4.	N2	C1	1.370(3)	1.365(3)

Table S3: Selected bond parameters for optimized **MPIT**, **DPPIT** and **TPPIT.**

Selected bond angles

S.no	Atom	Atom	Atom	**MPIT** (°)	**DPPIT** (°)	**TPPIT** (°)
1.	N1	C1	S1	129.13	129.07	129.02
2.	N2	C1	S1	127.11	127.13	127.13
3.	N2	C1	N1	103.76	103.80	103.85
4.	C1	N1	C2	124.74	124.42	124.23

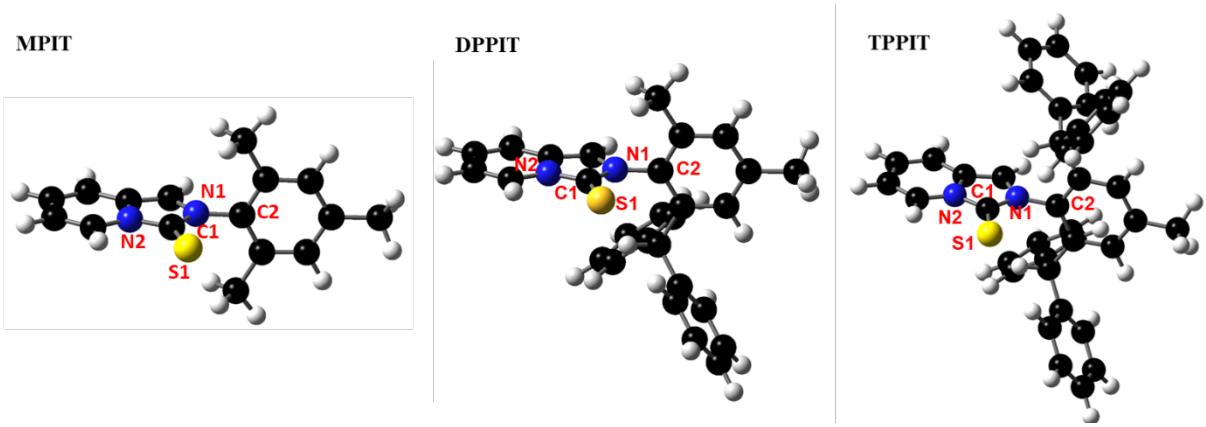

Selected bond distance

S.no.	Atom	Atom	**MPIT** (Å)	**DPPIT** (Å)	**TPPIT** (Å)
1.	S1	C1	1.6787	1.6810	1.6835
2.	N1	C2	1.4399	1.4402	1.4412
3.	N1	C1	1.3767	1.3781	1.3794
4.	N2	C1	1.3897	1.3873	1.3850

Table S4: Energy level of frontier molecular orbitals for **MPIT**, **DPPIT** and **TPPIT**.

Molecular Orbital	**MPIT** (eV)	**DPPIT** (eV)	**TPPIT** (eV)
LUMO+3	-0.9469561	-5.15655726	-5.227851089
LUMO+2	-0.400007	-5.197918566	-5.256695156
LUMO+1	-0.2312967	-5.234381821	-5.286355564
LUMO	-1.278118	-5.301593939	-5.32363516
HOMO	-4.70811	-7.225983014	-7.241765616
HOMO-1	-5.392207	-7.796333622	-7.800687443
HOMO-2	-6.50297	-9.090234929	-9.09132338
HOMO-3	-6.548419	-9.69759302	-9.759907089
E (LOMO-HUMO)	3.429994	1.924389074	1.918130456

Table S5: TD-DFT calculated oscillator strength and probable transition of **MPIT**.

Excited State	Energy (eV)	Wavelength (nm)	Osc. Strength	Major contribution
1	1.9224	638.30	0.0000	H-1 to L H to L
2	2.8251	438.87	0.0340	H to L (98%)
3	3.1297	396.16	0.0000	H-4 to L H to L+2 H to L+3
4	3.2762	378.44	0.0000	H-1 to L H to L+2
5	3.2787	372.57	0.0000	H-1 to L+2
6	3.7786	328.12	0.0000	H to L+1

Table S6: TD-DFT calculated oscillator strength and probable transition of **DPPIT**.

Excited State	Energy (eV)	Wavelength (nm)	Osc. Strength	Major contribution
1	2.8531	434.55	0.0332	H to L (98%)
2	3.3848	366.30	0.000	H-1 to L (98%)
3	3.7062	334.5318	0.0004	H to L+1 (96%) H toL+2 (2%)
4	3.8432	322.61	0.0052	H to L+1 (2%) H to L+2 (93%) H to L+4 (3%)
5	4.0415	306.78	0.003	H to L+3 (98%)
6	4.2333	292.88	0.011	H to L+2 (3%) H to L+4 (20%) H to L+5 (75%)

Table S7: TD-DFT calculated oscillator strength and probable transition of **TPPIT**.

Excited State	Energy (eV)	Wavelength (nm)	Osc. Strength	Major Contribution
1	2.8800	430.50	0.0311	H to L (98%)
2	3.4453	359.86	0.0000	H-1 to L (98%)
3	3.6346	341.12	0.0003	H to L+1 (98%)
4	3.7319	332.23	0.0026	H to L+2 (96%) H to L+6 (3%)
5	4.0187	308.52	0.0001	H to L+3 (99%)
6	4.0935	302.88	0.0048	H to L+4 (96%) H to L+6 (3%)
7	4.1200	300.93	0.0001	H to L+5 (99%)
8	4.2276	293.28	0.0464	H to L+2 (2%) H to L+6 (69%) H to L+7 (23%) H to L+11 (2%)